

---

# Adaptive Width Neural Networks

---

**Federico Errica**  
NEC Laboratories Europe

**Henrik Christiansen**  
NEC Laboratories Europe

**Viktor Zaverkin**  
NEC Laboratories Europe

**Mathias Niepert**  
University of Stuttgart  
NEC Laboratories Europe

**Francesco Alesiani**  
NEC Laboratories Europe

## Abstract

For almost 70 years, researchers have mostly relied on hyper-parameter tuning to select the width of neural networks' layers. This paper challenges the status quo by introducing an easy-to-use technique to learn an *unbounded* width of a neural network's layer *during training*. The technique does not rely on alternate optimization nor hand-crafted gradient heuristics; rather, it jointly optimizes the width and the parameters of each layer via simple backpropagation. We apply the technique to a broad range of data domains such as tables, images, text, sequences, and graphs, showing how the width adapts to the task's difficulty. The method imposes a soft ordering of importance among neurons, by which it also is possible to *truncate* the trained network at virtually zero cost, achieving a smooth trade-off between performance and compute resources in a structured way. Alternatively, one can dynamically compress the network with no performance degradation. In light of recent foundation models trained on large datasets, believed to require billions of parameters and where hyper-parameter tuning is unfeasible due to humongous training costs, our approach stands as a viable alternative for width learning.

## 1 Introduction

Since the construction of the Mark I Perceptron machine [48] the effective training of neural networks has remained an open research problem of great academic and practical value. The Mark I solved image recognition tasks by exploiting a layer of 512 *fixed* "association units" that in modern language correspond to the hidden units of a Multi-Layer Perceptron (MLP). MLPs possess universal approximation capabilities when assuming *arbitrary width* [10] and sigmoidal activations, and their convergence to good solutions was studied, for instance, in Rumelhart et al. [50] where the backpropagation algorithm was introduced as "simple, easy to implement on parallel hardware", and improvable by other techniques such as momentum that preserve locality of weight updates.

Yet, after almost 70 years of progress [34], the vast majority of neural networks, be they shallow or deep, still rely on a fixed choice of the number of neurons in their hidden layers. The width is typically treated as one of the many hyper-parameters that have to be carefully tuned whenever we approach a new task [62]. The tuning process has many names, such as model selection, hyper-parameter tuning, and cross-validation, and it is associated with non-negligible costs: Different architectural configurations are trained until one that performs best on a validation set is selected [41]. The configurations' space grows exponentially in the number of layers, so practitioners often resort to shortcuts such as picking a specific number of hidden units for *all* layers, which greatly reduces the search space together with the chances of selecting a better architecture for the task. Other techniques to tune hyper-parameters include constructive approaches [17, 64], which alternate parameter optimization and creation of new neurons, natural gradient-based heuristics that dynamically modify

the network [40], bi-level optimization [19], and neural architecture search [61], which often requires separate training runs for each configuration.

The hyper-parameters’ space exploration problem is exacerbated by the steep increase in size of recent neural architectures for language [9] and vision [68], for example, where parameters are in the order of billions to (supposedly) accommodate for a huge dataset. Training these models requires an amount of time, compute power, and energy that currently makes it unfeasible for most institutions to perform a thorough model selection and find good width parameters; the commonly accepted compromise is to stick to previously successful hyper-parameter choices. This may also explain why network pruning [6, 39], distillation [69] and quantization [39] techniques have recently been in the spotlight, as they trade-off hardware requirements and performance.

This work introduces a *simple* and *easy to use* technique to learn the width of each neural network’s layer without imposing upper bounds (we refer to it as **unbounded width**). The width of each layer is *dynamically* adjusted during backpropagation using the latest deep learning libraries [44], and it only requires a slight modification to the neural activations that does not alter the ability to parallelize computation. The technical strategy is to impose a soft ordering of hidden units by exploiting any monotonically decreasing function with unbounded support on natural numbers, which has a number of benefits. For instance, we do not need to fix a maximum number of neurons, which is typical of orthogonal approaches like supernetworks [61]. As a by-product, we can achieve a straightforward trade-off between parametrization and performance by removing the last rows/columns of weight matrices, which correspond to the “least important” neurons in the computation. Finally, we break symmetries in the parametrization of neural networks: it is not possible anymore to obtain an equivalent neural network behavior by permuting the weight matrices, which should in principle reduce the “jostling” effect where symmetric parametrizations compete when training starts [1].

We test our method on MLPs for tabular data, a Convolutional Neural Network (CNN) [33] for images, a Transformer architecture [58] for text, a Recurrent Neural Network (RNN) for sequences, for and a Deep Graph Network (DGN) [38, 52] for graphs, to showcase a broad scope of applicability. Empirical results show, as may be intuitively expected, that the width adapts to the task’s difficulty with the same performance of a fixed-width baseline. We also investigate compressing of the network at training time while preserving accuracy, as well as a post-hoc truncation inducing a controlled trade-off at zero additional cost. Ablations suggest that the learned width is not influenced by the starting width (under bounded activations) nor by the batch size, advocating for a potentially large reduction of the hyper-parameter configuration space.

## 2 Related Work

Constructive methods dynamically learn the width of neural networks and are related in spirit to this work. The cascade correlation algorithm [17] alternates standard training with the creation of a new hidden unit minimizing the neural network’s residual error. Similarly, the firefly network descent [64] grows the width and depth of a network every  $N$  training epochs via gradient descent on a dedicated loss. Yoon et al. [66] propose an ad-hoc algorithm for lifelong learning that grows the network by splitting and duplicating units to learn new tasks. Wu et al. [63] alternate training the network and then splitting existing neurons into offspring with equal weights. These works mostly focus on growing the neural network; Mitchell et al. [40] propose natural gradient-based heuristics to grow/shrink layers and hidden units of MLPs and CNNs. The main difference from our work is that we grow and shrink the network by simply computing the gradient of the loss, without relying on human-defined heuristics. The unbounded depth network of Nazaret and Blei [42], from which we draw inspiration, learns the number of layers of neural networks. Compared to that work, we focus our attention to the number of neurons, modifying the internals of the architecture rather than instantiating a multi-output one. Finally, we mention Bayesian nonparametrics approaches [43] that learn a potentially infinite number of clusters in an unsupervised fashion, as well as dynamic neural networks [24] that condition the architecture on input properties.

**Orthogonal Methods** Neural Architecture Search (NAS) is an automated process that designs neural networks for a given task [15, 61] and has been applied to different contexts [71, 35, 53]. Typically, neural network elements are added, removed, or modified based on validation performance [14, 60, 61], by means of reinforcement learning [70], evolutionary algorithms [47], and gradient-based approaches [35]. Typical NAS methods require enormous computational resources, sometimes

reaching thousands of GPU days [70], due to the retraining of each new configuration. While recent advances on one-shot NAS models [8, 45, 2, 4, 55, 54] have drastically reduced the computational costs, they mostly focus on CNNs, assume a bounded search space, and do not learn the width. As such, NAS methods are complementary to our approach. Bi-level optimization algorithms have also been used for hyper-parameter tuning [19], where hyper-parameters are the variables of the outer objective and the model parameters those of the inner objective. The solution sets of the inner problem are usually not available in closed form, which has been partly addressed by repeated application of (stochastic) gradient descent [11, 36, 18]. These methods are restricted to continuous hyper-parameters’ optimization, and cannot therefore be applied to width optimization.

Finally, pruning [6] and distillation [29] are two methods that reduce the size of neural networks by trading-off performances; the former deletes neural connections [39] or entire neurons [57, 12], the latter trains a smaller network (student) to mimic a larger one (teacher) [22]. In particular, dynamic pruning techniques can compress the network at training time [23], by applying hard or soft masks [28]; for a comprehensive survey on pruning, please refer to [27]. Compared to most pruning approaches, our work can delete connections *and* reduce the model’s memory, but also grow it indefinitely; compared to distillation, we do not necessarily need a new training to compress the network. These techniques, however, can be easily combined with our approach.

### 3 Adaptive Width Learning

We now introduce Adaptive Width Neural Networks (AWNN), a probabilistic framework that maximizes a simple variational objective via backpropagation over a neural network’s parameters.

We are given a dataset of  $N$  *i.i.d.* samples, with input  $x \in \mathbb{R}^F$ ,  $F \in \mathbb{N}^+$  and target  $y$  whose domain depends on whether the task is regression or classification. For samples  $X \in \mathbb{R}^{N \times F}$  and targets  $Y$ , the learning objective is to maximize the likelihood

$$\log p(Y|X) = \log \prod_{i=1}^N p(y_i|x_i) = \sum_{i=1}^N \log p(y_i|x_i) \quad (1)$$

with respect to the learnable parameters of  $p(y|x)$ . We define  $p(y|x)$  according to the graphical model of Figure 1 (left), to learn a neural network with **unbounded width** for each hidden layer  $\ell$ . To do so, we assume the existence of an **infinite** sequence of *i.i.d.* latent variables  $\theta_\ell = \{\theta_{\ell n}\}_{n=1}^\infty$ , where  $\theta_{\ell n}$  is a multivariate variable over the learnable weights of neuron  $n$  at layer  $\ell$ . However, since working with an infinite-width layer is not possible in practice, we also introduce a latent variable  $\lambda_\ell$  that samples how many neurons to use for layer  $\ell$ . That is, it *truncates an infinite width to a finite value* so that we can feasibly perform inference with the neural network. For a neural network of  $L$  layers, we define  $\theta = \{\theta_\ell\}_{\ell=1}^L$  and  $\lambda = \{\lambda_\ell\}_{\ell=1}^L$ , assuming independence across layers. Therefore, by marginalization one can write  $p(Y|X) = \int p(Y, \lambda, \theta|X) d\lambda d\theta$ . We then decompose the joint distribution using the independence assumptions of the graphical model:

$$p(Y, \lambda, \theta|X) = \prod_{i=1}^N p(y_i, \lambda, \theta|x_i) \quad p(y_i, \lambda, \theta|x_i) = p(y_i|\lambda, \theta, x_i) p(\lambda) p(\theta) \quad (2)$$

$$p(\lambda) = \prod_{\ell=1}^L p(\lambda_\ell) = \prod_{\ell=1}^L \mathcal{N}(\lambda_\ell; \mu_\ell^\lambda, \sigma_\ell^\lambda) \quad p(\theta) = \prod_{\ell=1}^L \prod_{n=1}^\infty p(\theta_{\ell n}) = \prod_{\ell=1}^L \prod_{n=1}^\infty \mathcal{N}(\theta_{\ell n}; \mathbf{0}, \text{diag}(\sigma_\ell^\theta)) \quad (3)$$

$$p(y_i|\lambda, \theta, x_i) = \text{Neural Network of Section 3.1} \quad (4)$$

where  $\sigma_\ell^\theta, \mu_\ell^\lambda, \sigma_\ell^\lambda$  are hyper-parameters. The neural network is parametrized by realizations  $\lambda \sim p(\lambda), \theta \sim \theta$  – it relies on a finite number of neurons as detailed later and in Section 3.1 – and it outputs either class probabilities (classification) or the mean of a Gaussian distribution (regression) to parametrize  $p(y_i|\lambda, \theta, x_i)$  depending on the task. Maximizing Equation (1), however, requires computing the integral  $\int p(Y, \lambda, \theta|X) d\lambda d\theta$ , which is intractable. Therefore, we turn to mean-field variational inference [30, 7] to maximize an expected lower bound (ELBO) instead. This requires to define a distribution over the latent variables  $q(\lambda, \theta)$  and re-phrase the objective as:

$$\log p(Y|X) \geq \mathbb{E}_{q(\lambda, \theta)} \left[ \log \frac{p(Y, \lambda, \theta|X)}{q(\lambda, \theta)} \right], \quad (5)$$

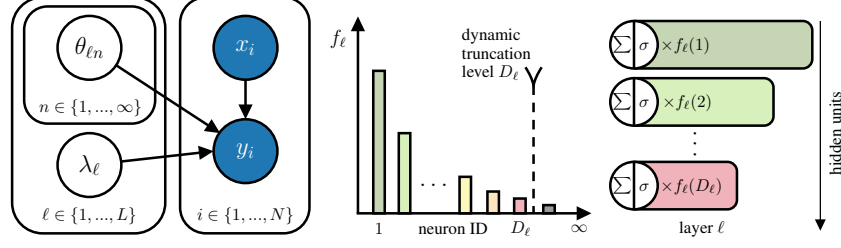


Figure 1: (Left) The graphical model of AWNN, with dark observable random variables and white latent ones. (Middle) The distribution  $f_\ell$  over hidden units' importance at layer  $\ell$  is parametrized by  $\lambda_\ell$ . The width of layer  $\ell$  is chosen as the quantile function of the distribution  $f_\ell$  evaluated at  $k$  and denoted by  $D_\ell$ . (Right) The hidden units' activations at layer  $\ell$  are rescaled by their importance.

where  $q(\boldsymbol{\lambda}, \boldsymbol{\theta})$  is parametrized by learnable *variational* parameters. Before continuing, we define the **truncated width**  $D_\ell$ , that is the finite number of neurons at layer  $\ell$ , as the quantile function evaluated at  $k$ , with  $k$  a hyper-parameter, of a distribution<sup>1</sup>  $f_\ell$  with infinite support over  $\mathbb{N}^+$  and parametrized by  $\lambda_\ell$ ; Appendix A and B provide formal requirements about  $f_\ell$ . In other words, we find the integer such that the cumulative mass function of  $f_\ell$  takes value  $k$ , and that integer  $D_\ell$  is the truncated width of layer  $\ell$ . *W.l.o.g.*, we implement  $f_\ell$  as a **discretized exponential distribution** adhering to Def. A.2, following the discretization strategy of Roy [49]: For every natural  $x$ , the discretized distribution relies on the exponential's cumulative distribution function:

$$f_\ell(x; \lambda_\ell) = (1 - e^{-\lambda_\ell(x+1)}) - (1 - e^{-\lambda_\ell x}). \quad (6)$$

We choose the exponential because it is a **monotonically decreasing** function and allows us to impose an ordering of importance among neurons, as detailed in Section 3.1.

Then, we can factorize the variational distribution  $q(\boldsymbol{\lambda}, \boldsymbol{\theta})$  into:

$$q(\boldsymbol{\lambda}, \boldsymbol{\theta}) = q(\boldsymbol{\lambda})q(\boldsymbol{\theta}|\boldsymbol{\lambda}) \quad q(\boldsymbol{\lambda}) = \prod_{\ell=1}^L q(\lambda_\ell) = \prod_{\ell=1}^L \mathcal{N}(\lambda_\ell; \nu_\ell, 1) \quad (7)$$

$$q(\boldsymbol{\theta}|\boldsymbol{\lambda}) = \prod_{\ell=1}^L \prod_{n=1}^{D_\ell} q(\theta_{\ell n}) \prod_{D_\ell+1}^{\infty} p(\theta_{\ell n}) \quad q(\theta_{\ell n}) = \mathcal{N}(\theta_{\ell n}; \text{diag}(\rho_{\ell n}), \mathbf{I}). \quad (8)$$

Here,  $\nu_\ell, \rho_{\ell n}$  are learnable variational parameters and, as before, we define  $\boldsymbol{\rho}_\ell = \{\rho_{\ell n}\}_{n=1}^{D_\ell}$ ,  $\boldsymbol{\rho} = \{\boldsymbol{\rho}_\ell\}_{\ell=1}^L$  and  $\boldsymbol{\nu} = \{\nu_\ell\}_{\ell=1}^L$ . Note that the set of variational parameters is **finite** as it depends on  $D_\ell$ .

By expanding Equation 5 using the above definitions and approximating the expectations at the first order, *i.e.*,  $\mathbb{E}_{q(\boldsymbol{\lambda})}[f(\boldsymbol{\lambda})] = f(\boldsymbol{\nu})$  and  $\mathbb{E}_{q(\boldsymbol{\theta}|\boldsymbol{\lambda})}[f(\boldsymbol{\theta})] = f(\boldsymbol{\rho})$  as in Nazaret and Blei [42], we obtain the final form of the ELBO<sup>2</sup> (the full derivation is in Appendix C):

$$\sum_{\ell}^L \log \frac{p(\nu_\ell; \mu_\ell^\lambda, \sigma_\ell^\lambda)}{q(\nu_\ell; \nu_\ell)} + \sum_{\ell}^L \sum_{n=1}^{D_\ell} \log \frac{p(\rho_{\ell n}; \sigma_\ell^\theta)}{q(\rho_{\ell n}; \rho_{\ell n})} + \sum_{i=1}^N \log p(y_i | \boldsymbol{\lambda} = \boldsymbol{\nu}, \boldsymbol{\theta} = \boldsymbol{\rho}, x_i), \quad (9)$$

where distributions' parameters are made explicit to distinguish them. The first two (optional) terms in the ELBO regularize the width of the layers and the magnitude of the parameters, respectively, whereas the third term accounts for the predictive performance.

In practice, the finite variational parameters  $\boldsymbol{\nu}, \boldsymbol{\rho}$  are those used to parametrize the neural network rather than sampling  $\boldsymbol{\lambda}, \boldsymbol{\theta}$ , which enables easy optimization via backpropagation. Maximizing Equation (9) will update each variational parameter  $\nu_\ell$ , which in turn will change the value of  $D_\ell$  **during training**. If  $D_\ell$  increases we initialize new neurons and draw their weights from a standard normal distribution, otherwise we discard the weights of the extra neurons. When implementing mini-batch training, the predictive loss needs to be rescaled by  $N/M$ , where  $M$  is the mini-batch size. From a Bayesian perspective, this is necessary as regularizers should weigh less if we have more data.

<sup>1</sup>General functions are allowed if a threshold can be computed.

<sup>2</sup>The higher  $k$  the better the ELBO approximation.

Finally, note that the first-order approximation leaves  $\nu$  and  $\rho$  completely free to change if not for the regularizers, that is, there is potentially no restriction imposed by the Gaussian assumptions.

Compared to a fixed-width network with weight decay, we need to choose the values of  $\mu_\ell^\lambda, \sigma_\ell^\lambda$ , as well as initialize the learnable  $\nu_\ell$ . The latter can be initially set to same value across layers since they can freely adapt later, or it can be sampled from the prior  $p(\lambda_\ell)$ . Therefore, we have two more hyper-parameters compared to the fixed-width network, but we make some considerations: **i**) it is always possible to use an uninformative prior over  $\lambda_\ell$ , removing the extra hyper-parameters letting the model freely adapt the width of each layer (as is typical of frequentist approaches); **ii**) the choice of higher level of hyper-parameters is known to be less stringent than that of hyper-parameters themselves [21, 5], so we do not need to explore many values of  $\mu_\ell^\lambda$  and  $\sigma_\ell^\lambda$ ; **iii**) our experiments suggest that AWNN can converge to similar widths regardless of the starting point  $\nu_\ell$ , so that we may just need to perform model selection over one/two sensible initial values.

### 3.1 Imposing a Soft Ordering on Neurons' Importance

Now that the learning objective has been formalized, the missing ingredient is the definition of the neural network  $p(y_i | \lambda = \nu, \theta = \rho, x_i)$  of Equation 4 as a modified MLP. Compared to a standard MLP, we need to make use of the variational parameters  $\nu$  that affect the truncation width at each hidden layer, whereas  $\rho$  are the weights. We chose a monotonically decreasing function  $f_\ell$ , thus when a new neuron is added its relative importance is low and will not drastically impact the network output and hidden activations. In other words, we impose a soft ordering of importance among neurons.

We simply modify the classical activation  $h_j^\ell$  of a hidden neuron  $j$  at layer  $\ell$  as

$$h_j^\ell = \sigma \left( \sum_{k=1}^{D_{\ell-1}} w_{jk}^\ell h_k^{\ell-1} \right) f_\ell(j; \nu_\ell), \quad (10)$$

where  $D_{\ell-1}$  is the truncated width of the previous layer,  $\sigma$  is a non-linear activation function and  $w_{jk}^\ell \in \rho_{\ell j}$ . That is, we rescale the activation of each neuron  $k$  by its ‘‘importance’’  $f_\ell(j; \nu_\ell)$ . Note that the bias parameter can be part of the weight vector as usual.

It is easy to see that, in theory, the optimization algorithm could rescale the weights of the next layer by a factor  $1/f_\ell(j; \nu_\ell)$  to compensate for the term  $f_\ell(j; \nu_\ell)$ . This could lead to a degenerate situation where the activations of the first neurons are small relative to the others, thus breaking the soft-ordering and potentially wasting neurons. There are two strategies to address this undesirable effect. The first is to regularize the magnitude of the weights thanks to the prior  $p(\theta_{\ell+1:n})$ , so that it may be difficult to compensate for the least important neurons that have a high  $1/f_\ell(j)$ . The second and less obvious strategy is to prevent the units’ activations of the current layer to compensate for high values by bounding their range, e.g., using a ReLU6 activation [51]. We apply both strategies to our experiments, although we noted that they do not seem strictly necessary in practice.

### 3.2 Rescaled Weight Initialization for Deep AWNN

Rescaling the activations of hidden units using Equation 10 causes activations of deeper layers to quickly decay to zero for an AWNN MLP with ReLU nonlinearity initialized using the well known Kaiming scheme [25]. This affects convergence since gradients get close to zero and it becomes impractical to train deep AWNN MLPs. We therefore derive a rescaled Kaiming weight that guarantees that the variance of activation across layers is constant at initialization.

**Theorem 3.1.** *Consider an MLP with activations as in Equation 10 and ReLU nonlinearity. At initialization, given  $\alpha_j^\ell = \sigma \left( \sum_{k=1}^{D_{\ell-1}} w_{jk}^\ell h_k^{\ell-1} \right)$ ,  $\text{Var}[w_{j*}^\ell] = \frac{2}{\sum_{j=1}^{D_{\ell-1}} f_\ell^2(j)} \Rightarrow \text{Var}[\alpha_j^\ell] \approx \text{Var}[\alpha_j^{\ell-1}]$ .*

*Proof.* See Appendix E for an extended proof.  $\square$

The extended proof shows there is a connection between the variance of activations and the variance of gradients. In particular, the sufficient conditions over  $\text{Var}[w_{j*}^\ell]$  are identical if one initializes  $\nu_\ell$  in the same way for all layers. Therefore, if we initialize weights from a Gaussian distribution with standard deviation  $\frac{\sqrt{2}}{\sqrt{\sum_{j=1}^{D_{\ell-1}} f_\ell^2(j)}}$ , we guarantee that at initialization the variance of the deep network’s gradients will be constant. The effect of the new initialization (dubbed ‘‘Kaiming+’’) can be seen in Figure

7, where the distribution of activation values at initialization does not collapse in subsequent layers. This change drastically impacts overall convergence on the SpiralHard synthetic dataset (described in Section 4), where it appears it would be otherwise hard to converge using a standard Kaiming initialization.

Algorithm 1 summarizes the main changes to the training procedure, namely the new initialization and the update of the model’s truncated width at each training step.

---

**Algorithm 1** AWNN Training Procedure

---

- 1: **Input:** Dataset  $\mathcal{D}$ , initialized AWNN model  $\mathcal{M}$  (Section 3.2)
  - 2: **Output:** Trained AWNN Model  $\mathcal{M}$
  - 3: **for** each training epoch **do**
  - 4:   **for** batch in  $\mathcal{D}$  **do**
  - 5:     update\_width( $\mathcal{M}$ )
  - 6:      $\hat{y} \leftarrow \mathcal{M}(\text{batch})$
  - 7:     loss  $\leftarrow$  ELBO( $\mathcal{M}$ , batch,  $\hat{y}$ ) // Eq. 9
  - 8:      $\mathcal{M} \leftarrow$  backpropagation( $\mathcal{M}$ , loss)
  - 9:   **function** update\_width( $\mathcal{M}$ ):
  - 10:     **for** layer  $\ell$  in  $\mathcal{M}.\text{hidden\_layers}$  **do**
  - 11:        $D_\ell \leftarrow$  quantile function of  $f_\ell(\cdot; \nu_\ell)$  evaluated at  $k$
  - 12:       Use  $D_\ell$  to update  $\rho_\ell, \rho_{\ell+1}$  // add/remove neurons
- 

### 3.3 Future Directions and Limitations

MLPs are ubiquitous in modern deep architectures. They are used at the very end of CNNs, in each Transformer layer, and they process messages coming from neighbors in DGNs. Our experiments focus on MLPs to showcase AWNN’s broad applicability, but there are many other scenarios where one can apply AWNN’s principles. For instance, one could impose a soft ordering of importance on CNNs’ filters at each layer, therefore learning the number of filters during training.

From a more theoretical perspective, we believe one could draw connections between our technique and the Information Bottleneck principle [56], which seeks maximally representative (i.e., performance) and compact representations (e.g., width). Finally, the analysis of different functions  $f$  to soft-order neurons, for instance a power-law distribution or a sigmoid-like function, may have a different impact on convergence and performance and could be empirically investigated.

AWNN needs to change the network at *training* time with an associated overhead. However, our current implementation has up to 3-4 $\times$  overhead *on the smallest datasets*, where the inference cost is negligible compared to the network update. Although this should not be an issue with more realistic tasks, especially if one considers the time spent testing different widths during grid search, further optimizations are conceivable: i) by updating the width every  $M$  mini-batches rather than at every step; ii) by allocating a larger network and dynamically grow it only if needed; iii) by creating ad-hoc support of AWNN on deep learning libraries like PyTorch.

## 4 Experiments and Setup

The purpose of the empirical analysis is **not** to claim AWNN is generally better than the fixed-width baseline. Rather, we demonstrate how AWNN overcomes the problem of fixing the number of neurons by learning it, thus reducing the amount of configurations to test. As such, due to the nature of this work and similarly to Mitchell et al. [40], we use the remaining space to thoroughly study the behavior of AWNN, so that it becomes clear how to use it in practice. We first quantitatively verify that AWNN does not harm the performance compared to baseline models and compare the chosen width by means of grid-search model selection with the learned width of AWNN. Second, we check that AWNN chooses a larger width for harder tasks, which can be seen as increasing the hypotheses space until the neural network finds a good path to convergence. Third, we verify that convergence speed is not significantly altered by AWNN, so that the main limitation lies in the extra overhead for adapting the network at each training step. As a sanity check, we study conditions under which AWNN’s learned width does not seem to depend on starting hyper-parameters, so that their choice does not matter much. Finally, we analyze other practical advantages of training a neural network under the AWNN framework: the ability to compress information during training or post training, and the resulting trade-offs. Further analyses are in the Appendix.

We compare baselines that undergo proper hyper-parameter tuning (called “Fixed”) against its AWNN version, where we replace any fixed MLP with an adaptive one. First, we train an MLP on 3 synthetic tabular tasks of increasing binary classification difficulty, namely a double moon, a spiral, and a double spiral that we call SpiralHard. A stratified hold-out split of 70% training/10% validation/20% test for risk assessment is chosen at random for these datasets. Similarly, we consider a ResNet-20

[26] trained on 3 image classification tasks, namely MNIST [32], CIFAR10, and CIFAR100 [31], where data splits and preprocessing are taken from the original paper and AWNN is applied to the downstream classifier. In the sequential domain, we implemented a basic adaptive Recurrent Neural Network (RNN) and evaluated on the PMNIST dataset [67] with the same data split as MNIST. In the graph domain, we train a Graph Isomorphism Network [65] on the NCI1 and REDDIT-B classification tasks, where topological information matters, using the same split and evaluation setup of Errica et al. [16]. Here, the first 1 hidden layer MLP as well as the one used in each graph convolutional layer are replaced by adaptive AWNN versions. On all these tasks, the metric of interest is the accuracy. Finally, for the textual domain we train a Transformer architecture [58] on the Multi30k English-German translation task [13], using a pretrained GPT-2 Tokenizer, and we evaluate the cross-entropy loss over the translated words. On tabular, image, and text-based tasks, an internal validation set (10%) for model selection is extracted from the union of outer training and validation sets, and the best configuration chosen according to the internal validation set is retrained 10 times on the outer train/validation/test splits, averaging test performances after an early stopping strategy on the validation set. Due to space reasons, we report datasets statistics and the hyper-parameter tried for the fixed and AWNN versions in Appendix F and G, respectively<sup>3</sup>. We ran the experiments on a server with 128 cores, 1.5TB of RAM, and 4 NVIDIA A40 with 46GB of memory.

## 5 Results

We begin by discussing the quantitative results of our experiments: Table 1 reports means and standard deviations across the 10 final training runs. In terms of performance, we observe that AWNN is more stable or accurate than a fixed MLP on DoubleMoon, Spiral, and SpiralHard; all other things being equal, it seems that using more neurons and their soft ordering are the main contributing factors to these improvements. On the image datasets, performances of AWNN are comparable to those of the fixed baseline but for CIFAR100, due to an unlucky run that did not converge. There, AWNN learns a smaller total width compared to grid search.

Results on graph datasets are interesting in two respects: First, the performance on REDDIT-B is significantly improved by AWNN both in terms of average performance and stability of results; second, the total learned width is significantly higher than those tried in Xu et al. [65], Errica et al. [16], meaning that a biased choice of possible widths had a profound influence on risk estimation for DGN models (i.e., GIN). This result makes it evident that it is important to let the network decide how many neurons are necessary to solve the task. Appendix H shows what happens when we retrain some fixed baselines using the total width as the width of each layer. Finally, the results on the Multi30k show that the AWNN Transformer learns to use 200x parameters less than the fixed Transformer for the feed-forward networks, achieving a statistically comparable test loss. This result is appealing when read through the lenses of modern deep learning, as the power required by some neural networks such as Large Language Models [9] is so high that cannot be afforded by most institutions, and it demands future investigations.

**Adaptation to Task Difficulty and Convergence** Intuitively, one would expect that AWNN learned larger widths for more difficult tasks. This is indeed what happens on the tabular datasets (and image datasets, see Appendix I) where some tasks are clearly harder than others. Figure 2 (left) shows that, given the same starting width per layer, the learned number of neurons grows according

Table 1: Performances and total width of MLP layers for the fixed and AWNN versions of the various models used. The exact width chosen by model selection on the graph datasets is unknown since we report published results. “Linear” means the chosen downstream classifier is a linear model.

	Fixed		AWNN		Width (Fixed)		Width (AWNN)	
	Mean	(Std)	Mean	(Std)	Mean	(Std)	Mean	(Std)
DoubleMoon	100.0	(0.0)	100.0	(0.0)	8	8.1	(2.8)	
Spiral	99.5	(0.5)	99.8	(0.1)	16	65.9	(8.7)	
SpiralHard	98.0	(2.0)	100.0	(0.0)	32	227.4	(32.4)	
MNIST	99.6	(0.1)	99.7	(0.0)	Linear	19.4	(4.8)	
CIFAR10	91.4	(0.2)	91.4	(0.2)	Linear	80.1	(12.4)	
CIFAR100	66.5	(0.4)	63.1	(4.0)	256	161.9	(57.8)	
PMNIST	91.1	(0.4)	95.7	(0.2)	24	806.3	(44.5)	
NCI1	80.0	(1.4)	80.0	(1.1)	(96-320)	731.3	(128.2)	
REDDIT-B	87.0	(4.4)	90.2	(1.3)	(96-320)	793.6	(574.0)	
Multi30k (↓)	1.43	(0.4)	1.51	(0.2)	24576	123.2	(187.9)	

<sup>3</sup>Code to reproduce results is in the supplementary material.

to the task’s difficulty. It is also interesting to observe that the total width for a multi-layer MLP on SpiralHard is significantly lower than that achieved by a single-layer MLP, which is consistent with the circuit complexity theory arguments put forward in Bengio et al. [3], Mhaskar et al. [37]. It also appears that convergence is not affected by the introduction of AWNN, as investigated in Figure 2 (right), which was not obvious considering the parametrization constraints encouraged by the rescaling of neurons’ activations.

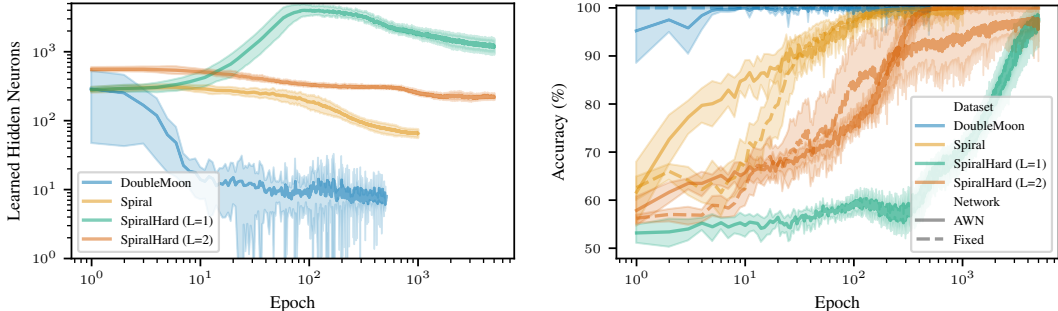


Figure 2: (Left) The learned width adapts to the increasing difficulty of the task, from the DoubleMoon to SpiralHard. (Right) AWNN reaches perfect test accuracy with a comparable amount of epochs on DoubleMoon and Spiral, while it converges faster on SpiralHard.

**Training Stability Analysis** To support our argument that AWNN can reduce the time spent performing hyper-parameter selection, we check whether AWNN learns a consistent amount of neurons across different training runs and hyper-parameter choices. Figure 3 reports the impact of the batch size and starting width averaged across the different configurations tried during model selection. Smaller batch sizes cause more instability, but in the long run we observe convergence to a similar width. Convergence with respect to different rates holds, instead, for the bounded ReLU6 activation; Appendix J shows that unbounded activations may cause the network to converge more slowly to the same width, which is in accord with the considerations about counterbalancing the rescaling effect of Section 3.1. Therefore, whenever possible, we recommend using bounded activations.

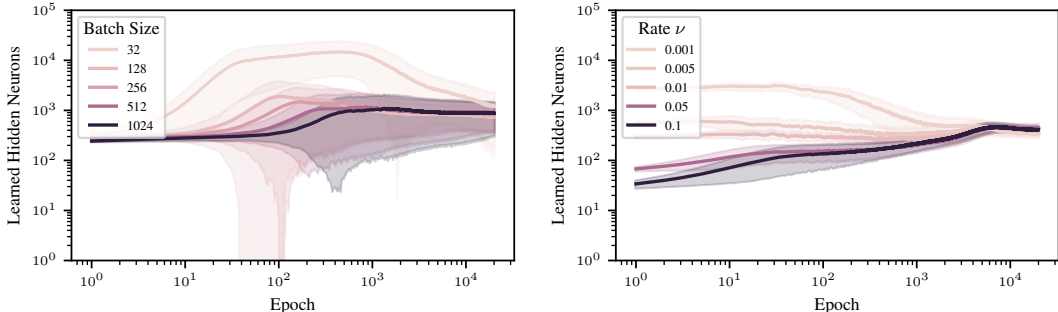


Figure 3: Training converges to similar widths on SpiralHard for different batch sizes (left) and starting rates  $\nu$ , but the latter seems to require a bounded nonlinearity such as ReLU6 to converge in a reasonable amount of epochs (right).

**Online Network Compression via Regularization** So far, we have used an uninformative prior  $p(\lambda)$  over the neural networks’ width. We demonstrate the effect of an informative prior by performing a width-annealing experiment on the SpiralHard dataset. We set an uninformative  $p(\theta)$  and ReLU6 nonlinearity. At epoch 1000, we introduce  $p(\lambda_\ell) = \mathcal{N}(\lambda_\ell; 0.05, 1)$ , and gradually anneal the standard deviation up to 0.1 at epoch 2500. Figure 4 shows that the width of the network reduces from approximately 800 neurons to 300 without any test performance degradation. We hypothesize that the least important neurons carry negligible information, therefore they can be safely removed without drastic changes in the output of the model. *This technique might be particularly useful to compress large models with billions of parameters.*

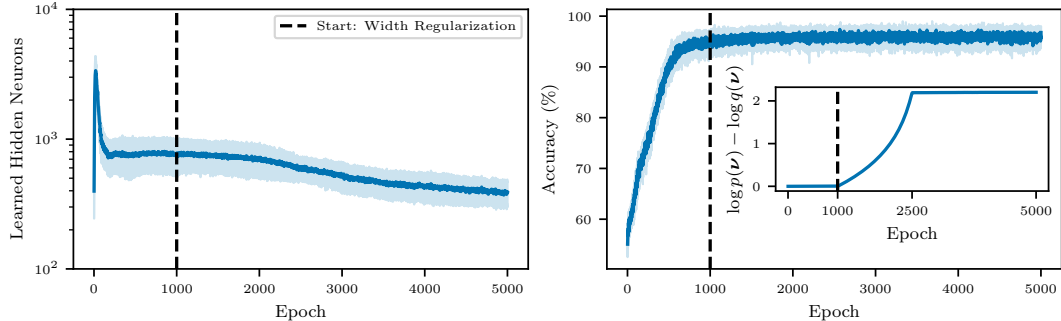


Figure 4: It is possible to regularize the width at training time by increasing the magnitude of the loss term  $\log \frac{p(\nu)}{q(\nu)}$ . The total width is reduced by more than 50% (left) while preserving accuracy (right). The inset plot refers to the loss term that AWNN tries to maximize.

**Post-hoc Truncation Achieves a Trade-off between Performance and Compute Resources** To further investigate the consequences of imposing a soft ordering among neurons, we show that it is possible to perform straightforward post-training truncation while still controlling the trade-off between performance and network size. Figure 5 shows an example for an MLP on the Spiral dataset, where the range of activation values (Equation 10) computed for all samples follows an exponential curve (right). Intuitively, removing the last neurons may have a negligible performance impact at the beginning and a drastic one as few neurons remain. This is what happens, where we are able to cut an MLP with hidden width 83 by 30% without loss of accuracy, after which a smooth degradation happens. If one accepts such a trade-off, this technique may be used to “distill” a trained neural network at virtually zero additional cost while reducing the memory requirements. Note that truncation heuristics that are either random or based on the magnitude of neurons’ activations (i.e., excluding the rescaling term) do not perform as well.

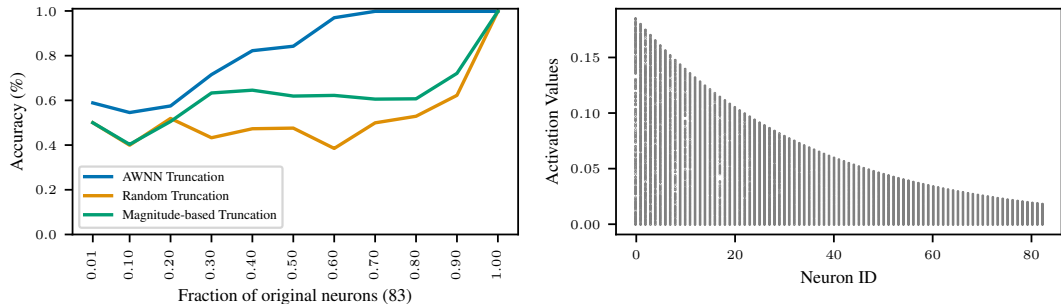


Figure 5: (Left) Thanks to the soft ordering imposed on the neurons, one can also truncate the neural network *after training* by simply removing the last neurons. (Right) The distribution of neurons’ activations for all Spiral test samples follows an exponential-like curve.

## 6 Conclusions

We introduced a new methodology to learn an unbounded width of neural network layers within a single training, by imposing a soft ordering of importance among neurons. Our approach requires very few changes to the architecture, adapts the width to the task’s difficulty, and does not impact negatively convergence. We showed stability of convergence to similar widths under bounded activations for different hyper-parameters configurations, advocating for a practical reduction of the width’s search space. A by-product of neurons’ ordering is the ability to easily compress the network during or after training, which is relevant in the context of foundational models trained on large data, which are believed to require billions of parameters. Finally, we have tested AWNN on different models and data domains to prove its broad scope of applicability: a Transformer architecture achieved a similar loss with 200x less parameters.

## References

- [1] David Barber. *Bayesian reasoning and machine learning*. Cambridge University Press, 2012.
- [2] Gabriel Bender, Pieter-Jan Kindermans, Barret Zoph, Vijay Vasudevan, and Quoc Le. Understanding and simplifying one-shot architecture search. In *Proceedings of the 35th International Conference on Machine Learning (ICML)*, 2018.
- [3] Yoshua Bengio, Pascal Lamblin, Dan Popovici, and Hugo Larochelle. Greedy layer-wise training of deep networks. In *Proceedings of the 20th Conference on Neural Information Processing Systems (NIPS)*, 2006.
- [4] Maxim Berman, Leonid Pishchulin, Ning Xu, Matthew B Blaschko, and Gérard Medioni. Aows: Adaptive and optimal network width search with latency constraints. In *Proceedings of the IEEE/CVF Conference on Computer Vision and Pattern Recognition (CVPR)*, 2020.
- [5] José M Bernardo and Adrian FM Smith. *Bayesian theory*, volume 405. John Wiley & Sons, 2009.
- [6] Davis Blalock, Jose Javier Gonzalez Ortiz, Jonathan Frankle, and John Guttag. What is the state of neural network pruning? In *Proceedings of machine learning and systems (MLSys)*, 2020.
- [7] David M Blei, Alp Kucukelbir, and Jon D McAuliffe. Variational inference: A review for statisticians. *Journal of the American statistical Association*, 112(518):859–877, 2017.
- [8] Andrew Brock, Theo Lim, J.M. Ritchie, and Nick Weston. SMASH: One-shot model architecture search through hypernetworks. In *6th International Conference on Learning Representations (ICLR)*, 2018.
- [9] Tom B. Brown, Benjamin Mann, Nick Ryder, Melanie Subbiah, Jared Kaplan, Prafulla Dhariwal, Arvind Neelakantan, Pranav Shyam, Girish Sastry, Amanda Askell, Sandhini Agarwal, Ariel Herbert-Voss, Gretchen Krueger, Tom Henighan, Rewon Child, Aditya Ramesh, Daniel M. Ziegler, Jeffrey Wu, Clemens Winter, Christopher Hesse, Mark Chen, Eric Sigler, Mateusz Litwin, Scott Gray, Benjamin Chess, Jack Clark, Christopher Berner, Sam McCandlish, Alec Radford, Ilya Sutskever, and Dario Amodei. Language models are few-shot learners. *arXiv preprint*, abs/2005.14165, 2020.
- [10] George Cybenko. Approximation by superpositions of a sigmoidal function. *Mathematics of control, signals and systems*, 2(4):303–314, 1989.
- [11] Justin Domke. Generic methods for optimization-based modeling. In *Proceedings of the 15th International Conference on Artificial Intelligence and Statistics (AISTATS)*, 2012.
- [12] Simon Dufort-Labbé, Pierluca D’Oro, Evgenii Nikishin, Razvan Pascanu, Pierre-Luc Bacon, and Aristide Baratin. Maxwell’s demon at work: Efficient pruning by leveraging saturation of neurons. *arXiv preprint*, 2024.
- [13] D. Elliott, S. Frank, K. Sima’an, and L. Specia. Multi30k: Multilingual english-german image descriptions. In *Proceedings of the 5th Workshop on Vision and Language*, 2016.
- [14] Thomas Elsken, Jan Hendrik Metzen, and Frank Hutter. Efficient multi-objective neural architecture search via lamarckian evolution. In *7th International Conference on Learning Representations (ICLR)*, 2019.
- [15] Thomas Elsken, Jan Hendrik Metzen, and Frank Hutter. Neural architecture search: A survey. *Journal of Machine Learning Research*, 20:1–21, 2019.
- [16] Federico Errica, Marco Podda, Davide Bacciu, and Alessio Micheli. A fair comparison of graph neural networks for graph classification. In *8th International Conference on Learning Representations (ICLR)*, 2020.
- [17] Scott Fahlman and Christian Lebiere. The cascade-correlation learning architecture. In *Proceedings of the 3rd Conference on Neural Information Processing Systems (NIPS)*, 1989.

- [18] Luca Franceschi, Michele Donini, Paolo Frasconi, and Massimiliano Pontil. Forward and reverse gradient-based hyperparameter optimization. In *Proceedings of the 34th International Conference on Machine Learning (ICML)*, 2017.
- [19] Luca Franceschi, Paolo Frasconi, Saverio Salzo, Riccardo Grazi, and Massimiliano Pontil. Bilevel programming for hyperparameter optimization and meta-learning. In *Proceedings of the 35th International Conference on Machine Learning (ICML)*, 2018.
- [20] Xavier Glorot and Yoshua Bengio. Understanding the difficulty of training deep feedforward neural networks. In *Proceedings of the 13th International Conference on Artificial Intelligence and Statistics (AISTATS)*, 2010.
- [21] Prem K. Goel and Morris H. Degroot. Information about hyperparameters in hierarchical models. *Journal of the American Statistical Association*, 76:140–147, 1981.
- [22] Jianping Gou, Baosheng Yu, Stephen J Maybank, and Dacheng Tao. Knowledge distillation: A survey. *International Journal of Computer Vision*, 129(6):1789–1819, 2021.
- [23] Yiwen Guo, Anbang Yao, and Yurong Chen. Dynamic network surgery for efficient dnns. *Advances in neural information processing systems*, 29, 2016.
- [24] Yizeng Han, Gao Huang, Shiji Song, Le Yang, Honghui Wang, and Yulin Wang. Dynamic neural networks: A survey. *IEEE transactions on pattern analysis and machine intelligence*, 44, 2021.
- [25] Kaiming He, Xiangyu Zhang, Shaoqing Ren, and Jian Sun. Delving deep into rectifiers: Surpassing human-level performance on imagenet classification. In *Proceedings of the IEEE international Conference on Computer Vision (ICCV)*, pages 1026–1034, 2015.
- [26] Kaiming He, Xiangyu Zhang, Shaoqing Ren, and Jian Sun. Deep residual learning for image recognition. In *Proceedings of the IEEE conference on Computer Vision and Pattern Recognition (CVPR)*, 2016.
- [27] Yang He and Lingao Xiao. Structured pruning for deep convolutional neural networks: A survey. *IEEE Transactions on Pattern Analysis and Machine Intelligence*, 46, 2023.
- [28] Yang He, Guoliang Kang, Xuanyi Dong, Yanwei Fu, and Yi Yang. Soft filter pruning for accelerating deep convolutional neural networks. In *Proceedings of the 27th International Joint Conference on Artificial Intelligence (IJCAI)*, 2018.
- [29] Geoffrey Hinton, Oriol Vinyals, and Jeff Dean. Distilling the knowledge in a neural network. *arXiv preprint*, 2015.
- [30] Michael I Jordan, Zoubin Ghahramani, Tommi S Jaakkola, and Lawrence K Saul. An introduction to variational methods for graphical models. *Machine learning*, 37:183–233, 1999.
- [31] Alex Krizhevsky. Learning multiple layers of features from tiny images. *Master’s thesis, University of Toronto*, 2009.
- [32] Yann LeCun. The mnist database of handwritten digits. <http://yann.lecun.com/exdb/mnist/>, 1998.
- [33] Yann LeCun, Bernhard Boser, John S Denker, Donnie Henderson, Richard E Howard, Wayne Hubbard, and Lawrence D Jackel. Backpropagation applied to handwritten zip code recognition. *Neural computation*, 1(4):541–551, 1989.
- [34] Yann LeCun, Yoshua Bengio, and Geoffrey Hinton. Deep learning. *nature*, 521(7553):436–444, 2015.
- [35] Hanxiao Liu, Karen Simonyan, and Yiming Yang. DARTS: Differentiable architecture search. In *7th International Conference on Learning Representations (ICLR)*, 2019.
- [36] Dougal Maclaurin, David Duvenaud, and Ryan Adams. Gradient-based hyperparameter optimization through reversible learning. In *Proceedings of the 32nd International Conference on Machine Learning (ICML)*, 2015.

- [37] Hrushikesh Mhaskar, Qianli Liao, and Tomaso Poggio. When and why are deep networks better than shallow ones? In *Proceedings of the AAAI conference on Artificial Intelligence (AAAI)*, 2017.
- [38] Alessio Micheli. Neural network for graphs: A contextual constructive approach. *IEEE Transactions on Neural Networks*, 20(3):498–511, 2009.
- [39] Asit Mishra, Jorge Albericio Latorre, Jeff Pool, Darko Stosic, Dusan Stosic, Ganesh Venkatesh, Chong Yu, and Paulius Micikevicius. Accelerating sparse deep neural networks. *arXiv preprint*, 2021.
- [40] Rupert Mitchell, Martin Mundt, and Kristian Kersting. Self expanding neural networks. *arXiv preprint*, 2023.
- [41] Tom Mitchell. *Machine learning*. McGraw-hill, 1997.
- [42] Achille Nazaret and David Blei. Variational inference for infinitely deep neural networks. In *Proceedings of the 39th International Conference on Machine Learning (ICML)*, 2022.
- [43] Peter Orbanz and Yee Whye Teh. Bayesian nonparametric models. *Encyclopedia of machine learning*, 1, 2010.
- [44] Adam Paszke, Sam Gross, Soumith Chintala, Gregory Chanan, Edward Yang, Zachary DeVito, Zeming Lin, Alban Desmaison, Luca Antiga, and Adam Lerer. Automatic differentiation in pytorch. In *Proceedings of the 31st Conference on Neural Information Processing Systems (NIPS)*, 2017.
- [45] Hieu Pham, Melody Guan, Barret Zoph, Quoc Le, and Jeff Dean. Efficient neural architecture search via parameters sharing. In *Proceedings of the 35th International Conference on Machine Learning (ICML)*, 2018.
- [46] Lutz Prechelt. Early stopping-but when? In *Neural Networks: Tricks of the trade*, pages 55–69. Springer, 1998.
- [47] Esteban Real, Alok Aggarwal, Yanping Huang, and Quoc V Le. Regularized evolution for image classifier architecture search. In *Proceedings of the 33rd AAAI Conference on Artificial Intelligence (AAAI)*, 2019.
- [48] Frank Rosenblatt. The perceptron: a probabilistic model for information storage and organization in the brain. *Psychological review*, 65(6):386, 1958.
- [49] Dilip Roy. The discrete normal distribution. *Communications in Statistics - Theory and Methods*, 32:1871–1883, 2003. doi: 10.1081/sta-120023256.
- [50] David E. Rumelhart, Geoffrey E. Hinton, and Ronald J. Williams. Learning representations by back-propagating errors. *Nature*, 323:533–536, 1986.
- [51] Mark Sandler, Andrew Howard, Menglong Zhu, Andrey Zhmoginov, and Liang-Chieh Chen. Mobilenetv2: Inverted residuals and linear bottlenecks. In *Proceedings of the IEEE Conference on Computer Vision and Pattern Recognition (CVPR)*, 2018.
- [52] Franco Scarselli, Marco Gori, Ah Chung Tsoi, Markus Hagenbuchner, and Gabriele Monfardini. The graph neural network model. *IEEE Transactions on Neural Networks*, 20(1):61–80, 2009.
- [53] David R So, Chen Liang, and Quoc V Le. The evolved transformer. In *Proceedings of the 36th International Conference on Machine Learning (ICML)*, 2019.
- [54] Xiu Su, Shan You, Tao Huang, Fei Wang, Chen Qian, Changshui Zhang, and Chang Xu. Locally free weight sharing for network width search. In *Proceedings of the 9th International Conference on Learning Representations (ICLR)*, 2021.
- [55] Xiu Su, Shan You, Fei Wang, Chen Qian, Changshui Zhang, and Chang Xu. Bcnet: Searching for network width with bilaterally coupled network. In *Proceedings of the IEEE/CVF Conference on Computer Vision and Pattern Recognition*, pages 2175–2184, 2021.

- [56] Naftali Tishby, Fernando C Pereira, and William Bialek. The information bottleneck method. *arXiv preprint*, 2000.
- [57] Lorenzo Valerio, Franco Maria Nardini, Andrea Passarella, and Raffaele Perego. Dynamic hard pruning of neural networks at the edge of the internet. *Journal of Network and Computer Applications*, 200:103330, 2022.
- [58] Ashish Vaswani, Noam Shazeer, Niki Parmar, Jakob Uszkoreit, Llion Jones, Aidan N Gomez, Lukasz Kaiser, and Illia Polosukhin. Attention is all you need. In *Proceedings of the 31st Conference on Neural Information Processing Systems (NIPS)*, 2017.
- [59] Aladin Virmaux and Kevin Scaman. Lipschitz regularity of deep neural networks: analysis and efficient estimation. *Advances in Neural Information Processing Systems*, 31, 2018.
- [60] Colin White, Sam Nolen, and Yash Savani. Local search is state of the art for nas benchmarks. In *Proceedings of the 37th Uncertainty in Artificial Intelligence Conference (UAI)*, 2021.
- [61] Colin White, Mahmoud Safari, Rhea Sukthanker, Binxin Ru, Thomas Elsken, Arber Zela, Debadeepta Dey, and Frank Hutter. Neural architecture search: Insights from 1000 papers. *arXiv preprint*, 2023.
- [62] David H Wolpert. The lack of a priori distinctions between learning algorithms. *Neural computation*, 8(7):1341–1390, 1996.
- [63] Lemeng Wu, Dilin Wang, and Qiang Liu. Splitting steepest descent for growing neural architectures. In *Proceedings of the 33rd Conference on Neural Information Processing Systems (NeurIPS)*, 2019.
- [64] Lemeng Wu, Bo Liu, Peter Stone, and Qiang Liu. Firefly neural architecture descent: a general approach for growing neural networks. In *Proceedings of the 34th Conference on Neural Information Processing Systems (NeurIPS)*, volume 33, 2020.
- [65] Keyulu Xu, Weihua Hu, Jure Leskovec, and Stefanie Jegelka. How powerful are graph neural networks? In *7th International Conference on Learning Representations (ICLR)*, 2019.
- [66] Jaehong Yoon, Eunho Yang, Jeongtae Lee, and Sung Ju Hwang. Lifelong learning with dynamically expandable networks. In *6th International Conference on Learning Representations (ICLR)*, 2018.
- [67] Friedemann Zenke, Ben Poole, and Surya Ganguli. Continual learning through synaptic intelligence. In *Proceedings of the 34th International Conference on Machine Learning (ICML)*, 2017.
- [68] Xiaohua Zhai, Alexander Kolesnikov, Neil Houlsby, and Lucas Beyer. Scaling vision transformers. In *Proceedings of the IEEE/CVF conference on Computer Vision and Pattern Recognition (CVPR)*, 2022.
- [69] Linfeng Zhang, Jiebo Song, Anni Gao, Jingwei Chen, Chenglong Bao, and Kaisheng Ma. Be your own teacher: Improve the performance of convolutional neural networks via self distillation. In *Proceedings of the IEEE/CVF International Conference on Computer Vision (ICCV)*, 2019.
- [70] Barret Zoph and Quoc V Le. Neural architecture search with reinforcement learning. In *4th International Conference on Learning Representations (ICLR)*, 2016.
- [71] Barret Zoph, Vijay Vasudevan, Jonathon Shlens, and Quoc V Le. Learning transferable architectures for scalable image recognition. *Proceedings of the IEEE conference on Computer Vision and Pattern Recognition (CVPR)*, 2018.

## A Background Notions

Since we were mostly inspired by the work of Nazaret and Blei [42], we complement the main text with an introduction to truncated distributions. In particular, by truncating a distribution at its quantile function evaluated at  $k$  (see Appendix B for a visual explanation), the support of the distribution becomes finite and countable, hence we can compute expectations in a finite number of steps. A truncated distribution should ideally satisfy some requirements defined in Nazaret and Blei [42] and illustrated below.

**Definition A.1.** A variational family  $Q = q(\omega)$  over  $\mathbb{N}^+$  is *unbounded* with *connected* and *bounded* members if

1.  $\forall q \in Q$ ,  $\text{support}(q)$  is bounded
2.  $\forall L \in \mathbb{N}^+, \exists q \in Q$  such that  $L \in \text{argmax}(q)$
3. Each parameter in the set  $\omega$  is a continuous variable.

The first condition allows us to compute the expectation over any  $q \in Q$  in finite time, condition 2 ensures there is a parametrization that assigns enough probability mass to each point in the support of  $q$ , and condition 3 is necessary for learning via backpropagation.

An important distinction with Nazaret and Blei [42] is that **we do not need nor want condition 2 to be satisfied**. As a matter of fact, we want to enforce a strict ordering of neurons where the first is always the most important one. Condition 2 is useful, as done in Nazaret and Blei [42], to assign enough ‘importance’ to a specific layer of an adaptive-depth architecture, while previous layers are still functional to the final result. In the context of adaptive-width networks, however, this mechanism may leave a lot of neurons completely unutilized, letting the network grow indefinitely. That is why we require that each distribution  $q$  is monotonically decreasing and all possible widths should have non-zero importance. We change the definition for the distributions we are interested in as follows:

**Definition A.2.** A variational family  $Q = q(\omega)$  over  $\mathbb{N}^+$  is *unbounded* with *connected*, *bounded*, and *decreasing* members if

1.  $\forall q \in Q$ ,  $\text{support}(q)$  is bounded
2.  $\forall q \in Q$ ,  $q$  is monotonically decreasing and  $\forall x \in \mathbb{N}^+, q(x) > 0$
3. Each parameter in the set  $\omega$  is a continuous variable.

## B How to Compute $D_\ell$ in Practice

To aid the understanding of how one computes  $D_\ell$ , we provide a visualization of the exponential distribution, its discretized version (Equation 6) and the quantile function evaluated at  $k = 0.9$  in Figure 6 below.

## C Full ELBO Derivation

The full ELBO derivation is as follows:

$$\mathbb{E}_{q(\lambda, \theta)} \left[ \log \frac{p(Y, \lambda, \theta | X)}{q(\lambda, \theta)} \right] = \tag{11}$$

$$\mathbb{E}_{q(\lambda)} \mathbb{E}_{q(\theta | \lambda)} [\log p(Y, \lambda, \theta | X) - \log q(\lambda, \theta)] = \tag{12}$$

$$\mathbb{E}_{q(\lambda)} \mathbb{E}_{q(\theta | \lambda)} [\log(p(Y | \lambda, \theta, X)p(\theta)p(\lambda)) - \log(q(\lambda)q(\theta | \lambda))] \tag{13}$$

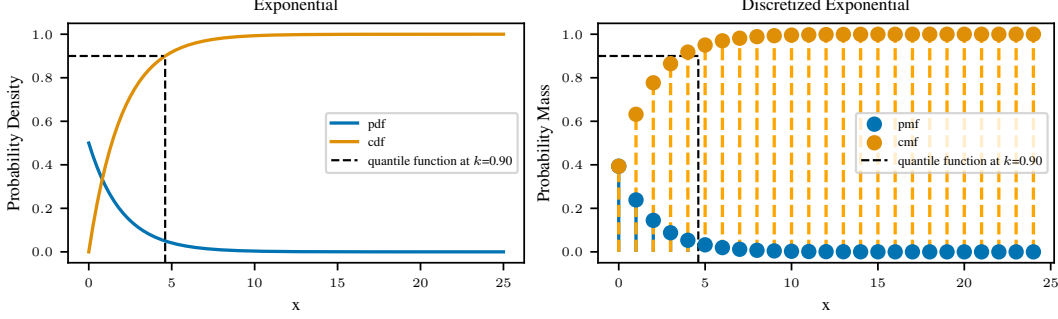


Figure 6: On the left, we provide a visualization of the exponential density with  $\lambda = 0.5$ , its cumulative density, and the quantile function evaluated at  $k = 0.9$ , which returns a value close to 5. On the right, we show the discretized exponential and its cumulative mass function; we can see that the quantile function of the continuous density provides an upper bound for the natural where the cumulative mass function is greater than  $k = 0.9$ . Therefore, one can safely use the ceiling of the output of the quantile function to determine the width  $D_\ell$  to use for a given value of  $\lambda$ .

where we factorized probabilities according to the independence assumptions of the graphical model. Then

$$\mathbb{E}_{q(\lambda)} \mathbb{E}_{q(\theta|\lambda)} [\log p(Y|\lambda, \theta, X) + \log p(\lambda) + \log p(\theta) - \log q(\lambda) - \log q(\theta|\lambda)] = \quad (14)$$

$$\mathbb{E}_{q(\lambda)} \mathbb{E}_{q(\theta|\lambda)} \left[ \log \frac{p(\lambda)}{q(\lambda)} + \log \frac{p(\theta)}{q(\theta|\lambda)} + \log p(Y|\lambda, \theta, X) \right] \approx \quad (15)$$

$$\log \frac{p(\nu)}{q(\nu)} + \log \frac{p(\rho)}{q(\rho|\nu)} + \log p(Y|\nu, \rho, X) \quad (16)$$

where we use the first-order approximation in the last step. Note that when computing  $\frac{p(\theta)}{q(\theta|\lambda)}$ , the products from  $D_{\ell+1}$  to infinity cancel out. Equation 13 follows by simply applying definitions, the iid assumption  $p(Y|\nu, \rho, X) = \prod_i^N p(y_i|\nu, \rho, x_i)$ , and by transforming products into summations using the logarithm.

An important note about the first-order (Taylor) approximation  $E_{q(\lambda;\nu)q(\theta|\lambda;\rho)}[f(\lambda, \theta)] \approx E_{q(\lambda;\nu)}[f(\lambda, \rho)] \approx f(\nu, \rho)$  is that the function  $f(\lambda, \theta) = \log \frac{p(\lambda)}{q(\lambda)} + \log \frac{p(\theta)}{q(\theta|\lambda)} + \log p(Y|\lambda, \theta, X)$  is not differentiable with respect to  $D_\ell$  when there is a jump in the quantile evaluated at  $k$ , so it would seem we cannot apply it. This also happens in Nazaret and Blei [42], Equation 11, when the function is a neural network containing non-differentiable activations like ReLU, but we could not find a discussion about it. Importantly, the function is not differentiable at a countable set of points (one for each possible width), which has a measure null. Since the Lebesgue integral of the expectation is over reals, we should be able to remove this set from the integral while ensuring that the approximation still holds mathematically.

## D Lipschitz Continuity of the ELBO

Whenever the quantile of the finite distribution changes, we need to change the number of neurons of the neural network. Here, we want to show that the change in the ELBO after a change in the number of neurons is bounded. Therefore, we provide a theoretical result (Proposition D.1) that shows that the ELBO satisfies the Lipschitz continuity.

**Proposition D.1** (AWN ELBO Lipschitz continuity). *The ELBO loss of Equation (9), with respect to the change in the depth  $D_\ell$  for the layer  $l$ , is Lipschitz continuous.*

*Proof.* We focus on the term involving  $D_\ell$  of the ELBO, we write Equation (9) as

$$\log \frac{p(\nu)}{q(\nu)} + \log \frac{p(\rho)}{q(\rho|\nu)} + \log p(Y|\nu, \rho, X)$$

where only the second and last terms depend on  $\mathbf{D} = \{D_\ell\}_{\ell=1}^L$ . Let's first define

$$\log \frac{p(\boldsymbol{\rho})}{q(\boldsymbol{\rho}|\boldsymbol{\nu})} = \sum_{\ell=1}^L \sum_{n=1}^{D_\ell} \log \frac{p(\rho_n^\ell)}{q(\rho_n^\ell|\boldsymbol{\nu})} = \sum_{\ell=1}^L f_1(D_\ell)$$

We have that  $f_1(D_\ell)$  is Lipschitz continuous, indeed, when  $D_\ell$  changes to  $D_{\ell'}$ , we have

$$|f_1(D_{\ell'}) - f_1(D_\ell)| = \left| \sum_{n=D_\ell}^{D_{\ell'}} \log \frac{p(\rho_n)}{q(\rho_n|\boldsymbol{\nu})} \right| \quad (17)$$

$$\leq \sum_{n=D_\ell}^{D_{\ell'}} \left| \log \frac{p(\rho_n)}{q(\rho_n|\boldsymbol{\nu})} \right| \quad (18)$$

$$\leq \max_n \left| \log \frac{p(\rho_n)}{q(\rho_n|\boldsymbol{\nu})} \right| |D_{\ell'} - D_\ell| \quad (19)$$

Therefore

$$|f_1(D_{\ell'}) - f_1(D_\ell)| \leq M |D_{\ell'} - D_\ell|$$

with  $M = \max_n \left| \log \frac{p(\rho_n)}{q(\rho_n|\boldsymbol{\nu})} \right|$ . We now look at the last term,

$$f_2(\mathbf{D}) = \log p(Y|\boldsymbol{\nu}, \boldsymbol{\rho}, X)$$

This function is a neural network followed by the squared norm. Therefore,  $f_2(\mathbf{D})$  is continuous almost everywhere [59], therefore Lipschitz on both parameters and the input. When we change  $D_\ell$  to  $D_{\ell'}$ , we are adding network parameters, in particular, if we look at the two-layer network, we have

$$y = V\sigma(Wx + b) + c, V \in \mathbb{R}^{m \times n}, W \in \mathbb{R}^{n \times d}$$

we then have new parameters, which can be shown to be

$$y' = V\sigma(Wx + b) + c + \underbrace{V'\sigma(W'x + b')}_{\text{new neurons}} + c', V' \in \mathbb{R}^{m \times n'}, W' \in \mathbb{R}^{n' \times d}, b' \in \mathbb{R}^{n'}, c' \in \mathbb{R}^m$$

the second term is also Lipschitz, therefore the function  $f_2(\mathbf{D})$  is also Lipschitz. Indeed the network is composed of a linear operation and the element-wise activation functions. If the activation functions are continuous and of bounded gradient, then the whole network is Lipschitz continuous.  $\square$

## E Full derivation of the rescaled weight initialization

This Section derives the formulas for the rescaled weight initialization both in the case of ReLU and activations like tanh.

**Background** We can rewrite Equation 10 as

$$h_i^\ell = \alpha_i^\ell p_i^\ell \quad (20)$$

$$\alpha_i^\ell = \sigma \left( \sum_{j=1}^{D_{\ell-1}} w_{ij}^\ell \underbrace{\alpha_j^{\ell-1} p_j^{\ell-1}}_{h_j^{\ell-1}} \right) \quad (21)$$

where  $p_i^\ell = f_\ell(i)$ .

As a refresher, the chain rule of calculus states that, given two differentiable functions  $g : \mathbb{R}^D \rightarrow \mathbb{R}$  and  $f = (f_1, \dots, f_D) : \mathbb{R} \rightarrow \mathbb{R}^D$ , their composition  $g \circ f : \mathbb{R} \rightarrow \mathbb{R}$  is differentiable and

$$\begin{aligned} (g \circ f)'(t) &= \nabla g(f(t))^T f'(t) \\ \nabla g(f(t)) &= \left( \frac{\partial g(f_1(t))}{\partial f_1(t)}, \dots, \frac{\partial g(f_D(t))}{\partial f_D(t)} \right) \in \mathbb{R}^{1 \times D} \\ f'(t) &= (f'_1(t), \dots, f'_D(t)) \in \mathbb{R}^{D \times 1} \end{aligned}$$

For reasons that will become clear later, we may want to compute the gradient of the loss function with respect to the intermediate activations  $\alpha^\ell$  at a given layer, that is  $\nabla \mathcal{L}(\alpha^\ell) = \left( \frac{\partial \mathcal{L}(\alpha_1^\ell)}{\partial \alpha_1^\ell}, \dots, \frac{\partial \mathcal{L}(\alpha_{N^\ell}^\ell)}{\partial \alpha_{N^\ell}^\ell} \right)$ .

We focus on the  $i$ -th partial derivative  $\frac{\partial \mathcal{L}(\alpha_i^\ell)}{\partial \alpha_i^\ell}$ , where the only variable is  $\alpha_i^\ell$ . Then, we view the computation of the loss function starting from  $\alpha_i^\ell$  as a composition of a function  $\alpha^{\ell+1} : \mathbb{R} \rightarrow \mathbb{R}^{N^{\ell+1}} = (\alpha_1^{\ell+1}(\alpha_i^\ell), \dots, \alpha_{N^{\ell+1}}^{\ell+1}(\alpha_i^\ell))$  and another function (abusing the notation)  $\mathcal{L} : \mathbb{R}^{N^{\ell+1}} \rightarrow \mathbb{R}$  that computes the loss value starting from  $\alpha^{\ell+1}$ . By the chain rule:

$$\underbrace{\frac{\partial \mathcal{L}(\alpha_i^\ell)}{\partial \alpha_i^\ell}}_{(g \circ f)'(t)} = \underbrace{\left( \frac{\partial \mathcal{L}(\alpha_1^{\ell+1})}{\partial \alpha_1^{\ell+1}}, \dots, \frac{\partial \mathcal{L}(\alpha_{N^{\ell+1}}^{\ell+1})}{\partial \alpha_{N^{\ell+1}}^{\ell+1}} \right)^T}_{\nabla g(f(t))^T} \underbrace{\left( \frac{\partial \alpha_1^{\ell+1}(\alpha_i^\ell)}{\partial \alpha_i^\ell}, \dots, \frac{\partial \alpha_{N^{\ell+1}}^{\ell+1}(\alpha_i^\ell)}{\partial \alpha_i^\ell} \right)}_{f'(t)} \quad (22)$$

**Theorem 3.1** *Let us consider an MLP with activations as in Equation 21. Let us also assume that the inputs and the parameters have been sampled independently from a Gaussian distribution with zero mean and variance  $\sigma^2 = \text{Var}[w_{ij}^\ell] \forall i, j, \ell$ . At initialization, the variance of the responses  $\alpha_i^\ell$  across layers is constant if,  $\forall \ell \in \{1, \dots, L\}$*

$$\text{Var}[w^\ell] = \frac{1}{\sum_j^{D_{\ell-1}} (p_j^{\ell+1})^2} \text{ for activation } \sigma \text{ such that } \sigma'(0) \approx 1 \quad (23)$$

$$\text{Var}[w^\ell] = \frac{2}{\sum_j^{D_{\ell-1}} (p_j^{\ell+1})^2} \text{ for the ReLU activation.} \quad (24)$$

In addition, we provide closed form formulas to to preserve the variance of the gradient across layers.

*Proof.* Let us start from the first case of  $\sigma'(0) \approx 1$ . Using the Taylor expansions for the moments of functions of random variables as in Glorot and Bengio [20]

$$\text{Var}[\alpha_i^\ell] = \text{Var} \left[ \sigma \left( \sum_{j=1}^{D_{\ell-1}} w_{ij}^\ell \alpha_j^{\ell-1} p_j^{\ell-1} \right) \right] \quad (25)$$

$$\approx \sigma' \left( \mathbb{E} \left[ \sum_{j=1}^{D_{\ell-1}} w_{ij}^\ell \alpha_j^{\ell-1} p_j^{\ell-1} \right] \right) \text{Var} \left[ \sum_{j=1}^{D_{\ell-1}} w_{ij}^\ell \alpha_j^{\ell-1} p_j^{\ell-1} \right] \quad (26)$$

Using the fact that  $p_j$  is a constant and that  $w$  and  $\alpha$  are independent from each other

$$\mathbb{E} \left[ \sum_{j=1}^{D_{\ell-1}} w_{ij}^\ell \alpha_j^{\ell-1} p_j^{\ell-1} \right] = \sum_{j=1}^{D_{\ell-1}} \underbrace{\mathbb{E}[w_{ij}^\ell]}_0 \mathbb{E}[\alpha_j^{\ell-1}] p_j^{\ell-1} = 0. \quad (27)$$

Therefore, recalling that  $\sigma'(0) \approx 1$

$$\sigma' \left( \mathbb{E} \left[ \sum_{j=1}^{D_{\ell-1}} w_{ij}^\ell \alpha_j^{\ell-1} p_j^{\ell-1} \right] \right) = 1. \quad (28)$$

As a result, we arrive at

$$\text{Var}[\alpha_i^\ell] \approx \text{Var} \left[ \sum_{j=1}^{D_{\ell-1}} w_{ij}^\ell \alpha_j^{\ell-1} p_j^{\ell-1} \right]. \quad (29)$$

Because  $w$  and  $\alpha$  are independent, they are also uncorrelated and their variances sum. Also, using the fact that  $\text{Var}[aX] = a^2 \text{Var}[X]$  for a constant  $a$ ,

$$\text{Var} \left[ \sum_{j=1}^{D_{\ell-1}} w_{ij}^\ell \alpha_j^{\ell-1} p_j^{\ell-1} \right] = \sum_{j=1}^{D_{\ell-1}} \text{Var} [w_{ij}^\ell \alpha_j^{\ell-1} p_j^{\ell-1}] = \sum_{j=1}^{D_{\ell-1}} \text{Var} [w_{ij}^\ell \alpha_j^{\ell-1}] (p_j^{\ell-1})^2 \quad (30)$$

Finally, because the mean of the independent variables involved is zero by assumption, it holds that  $\text{Var}[w_{ij}^\ell \alpha_j^{\ell-1}] = \text{Var}[w_{ij}^\ell] \text{Var}[\alpha_j^{\ell-1}]$ . We can also abstract from the indexes, since the weight variables are i.i.d. and from that it follows that  $\text{Var}[\alpha_i^\ell] = \text{Var}[\alpha_j^\ell] \forall i, j, i, j \in \{1, \dots, D_\ell\}$ , obtaining<sup>4</sup>

$$\text{Var}[\alpha^\ell] \approx \text{Var}[w^\ell] \text{Var}[\alpha^{\ell-1}] \sum_{j=1}^{D_{\ell-1}} (p_j^{\ell-1})^2, \quad (31)$$

noting again that the previous equation does not depend on  $i$ . We want to impose  $\text{Var}[\alpha^\ell] \approx \text{Var}[\alpha^{\ell-1}]$ , which can be achieved whenever

$$\text{Var}[w^\ell] \approx \frac{1}{\sum_{j=1}^{D_{\ell-1}} (p_j^{\ell-1})^2}. \quad (32)$$

**Condition on the gradients** From a backpropagation perspective, a similar desideratum would be to ensure that  $\text{Var}\left[\frac{\partial \mathcal{L}(\alpha_i^\ell)}{\partial \alpha_i^\ell}\right] = \text{Var}\left[\frac{\partial \mathcal{L}(\alpha_i^{\ell+1})}{\partial \alpha_i^{\ell+1}}\right]$ <sup>5</sup>.

Using Equation 22, and considering as in Glorot and Bengio [20] that at initialization we are in a linear regime where  $\sigma'(x) \approx 1$ ,

$$\text{Var}\left[\frac{\partial \mathcal{L}(\alpha_i^\ell)}{\partial \alpha_i^\ell}\right] = \text{Var}\left[\sum_{j=1}^{D_{\ell+1}} \frac{\partial \mathcal{L}(\alpha_j^{\ell+1})}{\partial \alpha_j^{\ell+1}} \frac{\partial \alpha_j^{\ell+1}(\alpha_i^\ell)}{\partial \alpha_i^\ell}\right] = \text{Var}\left[\sum_{j=1}^{D_{\ell+1}} \frac{\partial \mathcal{L}(\alpha_j^{\ell+1})}{\partial \alpha_j^{\ell+1}} \frac{\partial \alpha_j^{\ell+1}(\alpha_i^\ell)}{\partial \alpha_i^\ell}\right] \quad (33)$$

$$= \text{Var}\left[\sum_{j=1}^{D_{\ell+1}} \frac{\partial \mathcal{L}(\alpha_j^{\ell+1})}{\partial \alpha_j^{\ell+1}} \underbrace{\sigma'\left(\sum_{k=1}^{D_\ell} w_{jk}^{\ell+1} \alpha_k^\ell p_k^\ell\right)}_{\approx 1} w_{ji}^{\ell+1} p_i^\ell\right]. \quad (34)$$

Using the same arguments as above one can write

$$\text{Var}\left[\frac{\partial \mathcal{L}(\alpha_i^\ell)}{\partial \alpha_i^\ell}\right] \approx \text{Var}[w^{\ell+1}] \sum_{j=1}^{D_{\ell+1}} \text{Var}\left[\frac{\partial \mathcal{L}(\alpha_j^{\ell+1})}{\partial \alpha_j^{\ell+1}} p_i^\ell\right] = \text{Var}[w^{\ell+1}] (p_i^\ell)^2 \sum_{j=1}^{D_{\ell+1}} \text{Var}\left[\frac{\partial \mathcal{L}(\alpha_j^{\ell+1})}{\partial \alpha_j^{\ell+1}}\right]. \quad (35)$$

Expanding, we get

$$\text{Var}[w^{\ell+1}] (p_i^\ell)^2 \sum_{j=1}^{D_{\ell+1}} \text{Var}\left[\frac{\partial \mathcal{L}(\alpha_j^{\ell+1})}{\partial \alpha_j^{\ell+1}}\right] \quad (36)$$

$$= (p_i^\ell)^2 \left(\prod_{i=\ell+1}^{\ell+2} \text{Var}[w^{\ell+1}]\right) \sum_{j=1}^{D_{\ell+1}} (p_j^{\ell+1})^2 \underbrace{\left(\sum_{j'=1}^{D_{\ell+2}} \text{Var}\left[\frac{\partial \mathcal{L}(\alpha_{j'}^{\ell+2})}{\partial \alpha_{j'}^{\ell+2}}\right]\right)}_{\text{constant w.r.t. } j} \quad (37)$$

$$= (p_i^\ell)^2 \left(\prod_{i=\ell+1}^{\ell+2} \text{Var}[w^{\ell+1}]\right) \left(\sum_{j'=1}^{D_{\ell+2}} \text{Var}\left[\frac{\partial \mathcal{L}(\alpha_{j'}^{\ell+2})}{\partial \alpha_{j'}^{\ell+2}}\right]\right) \left(\sum_{j=1}^{D_{\ell+1}} (p_j^{\ell+1})^2\right) \quad (38)$$

Therefore, we can recursively expand these terms and obtain

$$\text{Var}\left[\frac{\partial \mathcal{L}(\alpha_i^\ell)}{\partial \alpha_i^\ell}\right] = (p_i^\ell)^2 \left(\prod_{k=\ell+1}^L \text{Var}[w^k]\right) \left(\sum_{j'=1}^{D_L} \text{Var}\left[\frac{\partial \mathcal{L}(\alpha_{j'}^{D_L})}{\partial \alpha_{j'}^{D_L}}\right]\right) \left(\prod_{k=\ell+1}^{L-1} \sum_{j_k=1}^{D_k} (p_{j_k}^k)^2\right). \quad (39)$$

<sup>4</sup>It is worth noting that, in standard MLPs,  $p_j^\ell = 1$  so we recover the derivation of Glorot and Bengio [20], since  $\sum_{j=1}^{D_{\ell-1}} (p_j^{\ell-1})^2$  would be equal to  $D_{\ell-1}$ . In Glorot and Bengio [20] our  $D_{\ell-1}$  is denoted as “ $n_{\ell'}$ ” (see Equation 5).

<sup>5</sup>Note that what we impose is different from Glorot and Bengio [20], where the specific position  $i$  is irrelevant. Here, we are asking that the variance of the gradients for neurons in the same position  $i$ , but at different layers, stays constant. Alternatively, we could impose an equivalence for all  $i \neq i'$ .

In this case, the variance depends on  $i$  just for the term  $(p_i^\ell)^2$ . Finally, by imposing

$$\text{Var} \left[ \frac{\partial \mathcal{L}(\alpha_i^\ell)}{\partial \alpha_i^\ell} \right] = \text{Var} \left[ \frac{\partial \mathcal{L}(\alpha_i^{\ell+1})}{\partial \alpha_i^{\ell+1}} \right] \quad (40)$$

and simplifying common terms we obtain

$$(p_i^\ell)^2 \text{Var}[w^{\ell+1}] \left( \sum_{j=1}^{D_{\ell+1}} (p_j^{\ell+1})^2 \right) = (p_i^{\ell+1})^2 \quad (41)$$

$$\text{Var}[w^{\ell+1}] = \frac{(p_i^{\ell+1})^2}{(p_i^\ell)^2 \sum_{j=1}^{D_{\ell+1}} (p_j^{\ell+1})^2}. \quad (42)$$

Both Equations 32 and 42 are verified when we initialize the distributions  $f_\ell$  in the same way for all layers, which implies  $(p_i^\ell)^2 = (p_i^{\ell+1})^2$ . Note that without this last requirement, Equation 42 would violate the i.i.d. assumption of the weights.

To show a similar initialization for ReLU activations, we need the following lemma.

**Lemma E.1.** *Consider the ReLU activation  $y = \max(0, x)$  and a symmetric distribution  $p(x)$  around zero. Then  $\mathbb{E}[y^2] = \frac{1}{2} \text{Var}[x]$ .*

*Proof.*

$$\mathbb{E}[y^2] = \int_{-\infty}^{+\infty} \max(0, x)^2 p(x) dx = \int_0^{+\infty} x^2 p(x) dx = \frac{1}{2} \int_{-\infty}^{+\infty} x^2 p(x) dx \quad (43)$$

Because  $p(x)$  is symmetric,  $\mathbb{E}[x] = 0$ . Then

$$\frac{1}{2} \int_{-\infty}^{+\infty} x^2 p(x) dx = \frac{1}{2} \int_{-\infty}^{+\infty} (x - \mathbb{E}[x])^2 p(x) dx = \frac{1}{2} \text{Var}[x]. \quad (44)$$

□

Using Lemma E.1, we can rewrite Equation 26 as

$$\text{Var}[\alpha_i^\ell] = \text{Var} \left[ \sigma \left( \sum_{j=1}^{D_{\ell-1}} w_{ij}^\ell \alpha_j^{\ell-1} p_j^{\ell-1} \right) \right] = \frac{1}{2} \text{Var} \left[ \sum_{j=1}^{D_{\ell-1}} w_{ij}^\ell \alpha_j^{\ell-1} p_j^{\ell-1} \right] \quad (45)$$

$$= \frac{1}{2} \text{Var}[w^\ell] \text{Var}[\alpha^{\ell-1}] \sum_{j=1}^{D_{\ell-1}} (p_j^{\ell-1})^2 \quad (46)$$

where no approximation has been made. Similar to prior results, it follows that

$$\text{Var}[w^\ell] = \frac{2}{\sum_{j=1}^{D_{\ell-1}} (p_j^{\ell-1})^2}. \quad (47)$$

From a backpropagation perspective, since  $\sigma'(x) \approx 1$ , we use similar arguments as in He et al. [25]: we assume that the pre-activations  $\alpha$  have zero mean, then the derivative of the ReLU can have values zero or one with equal probability. One can show, by expanding the definition of variance, that  $\text{Var}[\sigma' \left( \sum_{k=1}^{D_\ell} w_{jk}^{\ell+1} \alpha_k^\ell p_k^\ell \right) w_{ji}^{\ell+1}] = \frac{1}{2} \text{Var}[w_{ji}^{\ell+1}]$ . As a result, one can re-write Equation 26 as

$$\text{Var} \left[ \sum_{j=1}^{D_{\ell+1}} \frac{\partial \mathcal{L}(\alpha_j^{\ell+1})}{\partial \alpha_j^{\ell+1}} \sigma' \left( \sum_{k=1}^{D_\ell} w_{jk}^{\ell+1} \alpha_k^\ell p_k^\ell \right) w_{ji}^{\ell+1} p_i^\ell \right] \quad (48)$$

$$\approx \frac{1}{2} \text{Var}[w^{\ell+1}] (p_i^\ell)^2 \sum_{j=1}^{D_{\ell+1}} \text{Var} \left[ \frac{\partial \mathcal{L}(\alpha_j^{\ell+1})}{\partial \alpha_j^{\ell+1}} \right], \quad (49)$$

where we have made the assumption of independence between  $\sigma' \left( \sum_{k=1}^{D_\ell} w_{jk}^{\ell+1} \alpha_k^\ell p_k^\ell \right)$  and  $w_{ji}^{\ell+1}$  since the former term is likely a constant. Following an identical derivation as above, we obtain

$$\text{Var}[w^{\ell+1}] = \frac{2(p_i^{\ell+1})^2}{(p_i^\ell)^2 \sum_{j=1}^{D_{\ell+1}} (p_j^{\ell+1})^2} \quad (50)$$

which is almost identical to Equation 47 and not dependent on  $i$  when we initialize  $f_\ell$  in the same way for all layers.  $\square$

**Comparison of convergence for different initializations** Below, we provide a comparison of convergence between an AWNN ReLU MLP initialized with the standard Kaiming scheme and one initialized according to our theoretical results (“Kaiming+”).

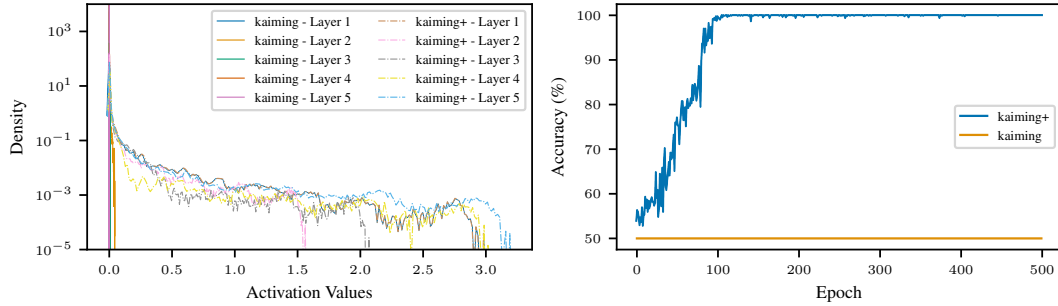


Figure 7: (Left) Effect of the rescaled initialization scheme (“Kaiming+”) on a ReLU-based MLP, where neurons’ activations are computed using Equation 10. Compared to the standard initialization, the variance of activations agrees with the theoretical result. (Right) Without the rescaled initialization, convergence is hard to attain on the SpiralHard dataset (please refer to the next section for details about the dataset).

## F Dataset Info and Statistics

The synthetic datasets DoubleMoon, Spiral, and SpiralHard are shown in Figure 8. These binary classification datasets have been specifically created to analyze the behavior of AWNN in a controlled scenario where we are sure that the difficulty of the task increases. We provide the code to generate these datasets in the supplementary material.

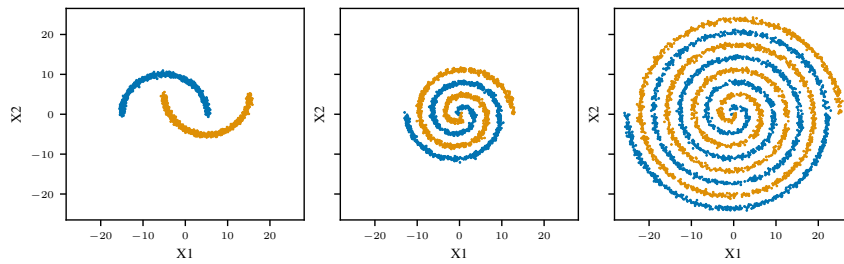


Figure 8: The DoubleMoon, Spiral, and SpiralHard synthetic datasets are used to test AWNN’s inner workings, and are ordered difficulty. Orange and blue colors denote different classes.

Table 2 reports information on their base statistics and the data splits created to carry out model selection (inner split) and risk assessment (outer split), respectively. Note that for Multi30k, the maximum sequence length is 128 and the number of possible tokens is 50527. The classification loss is computed by comparing the predicted token against the expected one, ignoring any token beyond the length of the actual target. For a detailed description of the graph datasets, the reader can refer to Errica et al. [16].

Table 2: Dataset statistics and number of samples in each split are shown.

	# Samples	# Features	# Classes	Outer Split (TR/VL/TE)	Inner Split (TR/VL)
DoubleMoon	2500	2	2	1750/250/500	1800/200
Spiral	2500	2	2	1750/250/500	1800/200
SpiralHard	5000	2	2	3500/500/1000	3600/400
MNIST	70000	28x28	10	53000/7000/10000	54000/6000
CIFAR10	60000	32x32x3	10	44000/6000/10000	45000/5000
CIFAR100	60000	32x32x3	100	44000/6000/10000	45000/5000
NCI1	4110	37	2	3288/411/411	3329/370
REDDIT-B	2000	1	2	1800/100/100	1710/190
Multi30k	31000	128x50257	Multilabel	29000/1000/1000	29000/1000

## G Hyper-parameters for fixed and AWNN models

For each data domain, we discuss the set of hyper-parameters tried during model selection for the fixed baseline and for AWNN. We try our best to keep architectural choices identical with the exception of the width of the MLPs used by each model. In all experiments, we either run patience-based early stopping [46] or simply select the epoch with best validation score.

### G.1 Synthetic Tabular Datasets and Permuted MNIST

We report the hyper-parameter configurations tried for the fixed MLP/RNN and AWNN in Table 3. In particular, the starting width of AWNN under the quantile function evaluated at  $k = 0.9$  is approximately 256 hidden neurons. We also noticed that a learning rate value of 0.1 makes learning the width unstable, so we did not use it in our experiments. The total number of configurations for the fixed models is 180, for AWNN is 18. We also did not impose any prior on an expected size to see if AWNN recovers a similar width compared to the best fixed model (please refer to Table 1) starting from the largest configuration among the fixed models.

Table 3: Hyper-parameter configurations for standard MLP/RNN and AWNN versions on tabular datasets.

Hyper-Parameter	DoubleMoon	Spiral	SpiralHard
Batch Size	32	[32, 128] (MLP/RNN), 128 (AWNN)	[32, 128] (MLP/RNN), 128 (AWNN)
Epochs	500	1000	5000
Hidden Layers	1	1	[1, 2, 4]
Layer Width		[8, 16, 24, 128, 256]	
Non-linearity		[ReLU, LeakyReLU, ReLU6]	
Optimizer		Adam, learning rate $\in [0.1, 0.01]$ (MLP/RNN), 0.01 (AWNN)	
<b>AWNN Specific</b>			
Quantile Fun. Threshold $k$		0.9	
Exponential Distributions Rate		0.01	
$\sigma_\ell^\theta$		[1.0, 10.0]	
Prior over $\lambda$		Uninformative	

### G.2 Image Classification Datasets

We train from scratch a ResNet20 and focus our architectural choices on the MLP that performs classification using the flattened representation provided by the previous CNN layers. This ensures that any change in performance is only due to the changes we apply to the MLP. The configurations are shown in Table 4; note that a width of 0 implies a linear classifier instead of a 1 hidden layer MLP. After previous results on tabular datasets showed that a LeakyReLU performs very well, we fixed it in the rest of the experiments. In this case, we test 5 different configurations of the fixed baseline, whereas we do not have to perform any model selection for AWNN. The rate of the exponential distribution has been chosen to have a starting width of approximately 128 neurons, which is the median value among the ones tried for the fixed model.

Table 4: Hyper-parameter configurations for standard MLP and AWNN versions on image classification datasets.

Hyper-Parameter	MNIST / CIFAR10 / CIFAR100
Batch Size	128
Epochs	200
Layer Width (classification layer)	[0, 32, 128, 256, 512]
Optimizer	SGD, learning rate 0.1, weight decay 0.0001, momentum 0.9
Scheduler	Multiply learning rate by 0.1 at epochs 50, 100, 150
<b>AWNN Specific</b>	
Quantile Fun. Threshold $k$	0.9
Exponential Distributions Rate	0.02
$\sigma_\ell^\theta$	1.0
Prior over $\lambda$	Uninformative

### G.3 Text Translation Tasks

Due to the cost of training a Transformer architecture from scratch on a medium size dataset like Multi30k, we use most hyper-parameters’ configurations of the base Transformer in Vaswani et al. [58], with the difference that AWNN is applied to the MLPs in each encoder and decoder layer. We train an architecture with 6 encoder and 6 decoder layers for 500 epochs, with a patience of 250 epochs applied to the validation loss. We use an Adam optimizer with learning rate 0.01, weight decay  $5e-4$ , and epsilon  $5e-9$ . We also introduce a scheduler that reduces the learning rate by a factor 0.9 when a plateau in the loss is reached. The number of attention heads is set to 8 and the dropout to 0.1. We try different widths for the MLPs, namely [128,256,512,1024,2048]. The embedding size is fixed to 512 and the batch size is 128. The AWNN version starts with an exponential distribution rate of 0.004, corresponding to approximately 512 neurons, and a  $\sigma_\ell^\alpha=1$ .

### G.4 Graph Classification Tasks

We train the AWNN version of Graph Isomorphism Network, following the setup of Errica et al. [16] and reusing the published results. We test 12 configurations as shown in the table below. Please note that an extra MLP with 1 hidden layer is always placed before the sequence of graph convolutional layers.

Table 5: Hyper-parameter configurations for AWNN versions on graph classification datasets.

Hyper-Parameter	NCII / REDDIT-B
Batch Size	[32,128]
Epochs	1000
Graph Conv. Layers	[1, 2, 4]
Global Pooling	[sum, mean]
Optimizer	Adam, learning rate 0.01
<b>AWNN Specific</b>	
Patience	500 epochs
Quantile Fun. Threshold $k$	0.9
Exponential Distributions Rate	0.02
$\sigma_\ell^\theta$	10.0
Prior over $\lambda$	Uninformative

## H Re-training a fixed network with the learned width

While on DoubleMoon AWNN learns a similar number of neurons chosen by the model selection procedure and the convergence to the perfect solution over 10 runs seem much more stable, this is not the case on Spiral, SpiralHard and REDDIT-B, where AWNN learns a higher total width over

layers. To investigate whether the width learned by AWNN on these datasets is indeed the reason behind the better performances (either a more stable training or better accuracy), we run again the experiments on the baseline networks, this time by fixing the width of each layer to the average width over hidden layers learned by AWNN and reported in Table 1. We call this experiment “Fixed+”.

	Spiral	SpiralHard	REDDIT-B
Fixed	99.5(0.5)	98.0(2.0)	87.0(4.4)
AWNN	99.8(0.1)	100.0(0.0)	90.2(1.3)
Fixed+	100.0(0.1)	83.2(17.0)	90.7(1.4)

The results suggest that by using more neurons than those selected by grid search – possibly because the validation results were identical between different configurations – it is actually possible to improve both accuracy and stability of results on Spiral and REDDIT-B, while we had a convergence issue on SpiralHard. Notice that the number of neurons learned by AWNN on REDDIT-B was well outside of the range investigated by Xu et al. [65] and Errica et al. [16], demonstrating that the practitioner’s bias can play an important role on the final performance.

### I Further qualitative results on image classification datasets

Because it is well known that MNIST, CIFAR10, and CIFAR100 are datasets of increasing difficulty, we attach a figure depicting the learned number of neurons and the convergence of AWNN on these datasets, following the practices highlighted in He et al. [26] and described in Table 4 to bring the ResNet20 to convergence. Akin to the tabular datasets, we see a clear pattern where the learned number of neurons, averaged over the 10 final training runs, increases together with the task difficulty. The AWNN version of the ResNet20 converges in the same amount of epochs as the fixed one.

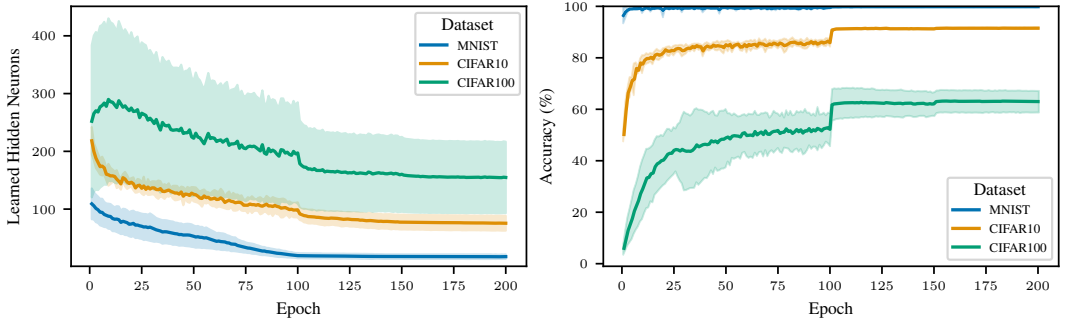


Figure 9: We present an analysis similar to Figure 2 but for image classification datasets of increasing difficulty. One can observe the jumps caused by the learning rate’s scheduling strategy.

## J Non-linearity ablation study

Below, we report an ablation study on the impact of non-linear activation functions. We analyze the convergence to the same width across different batch sizes and exponential starting rates  $\lambda$  on the SpiralHard dataset.

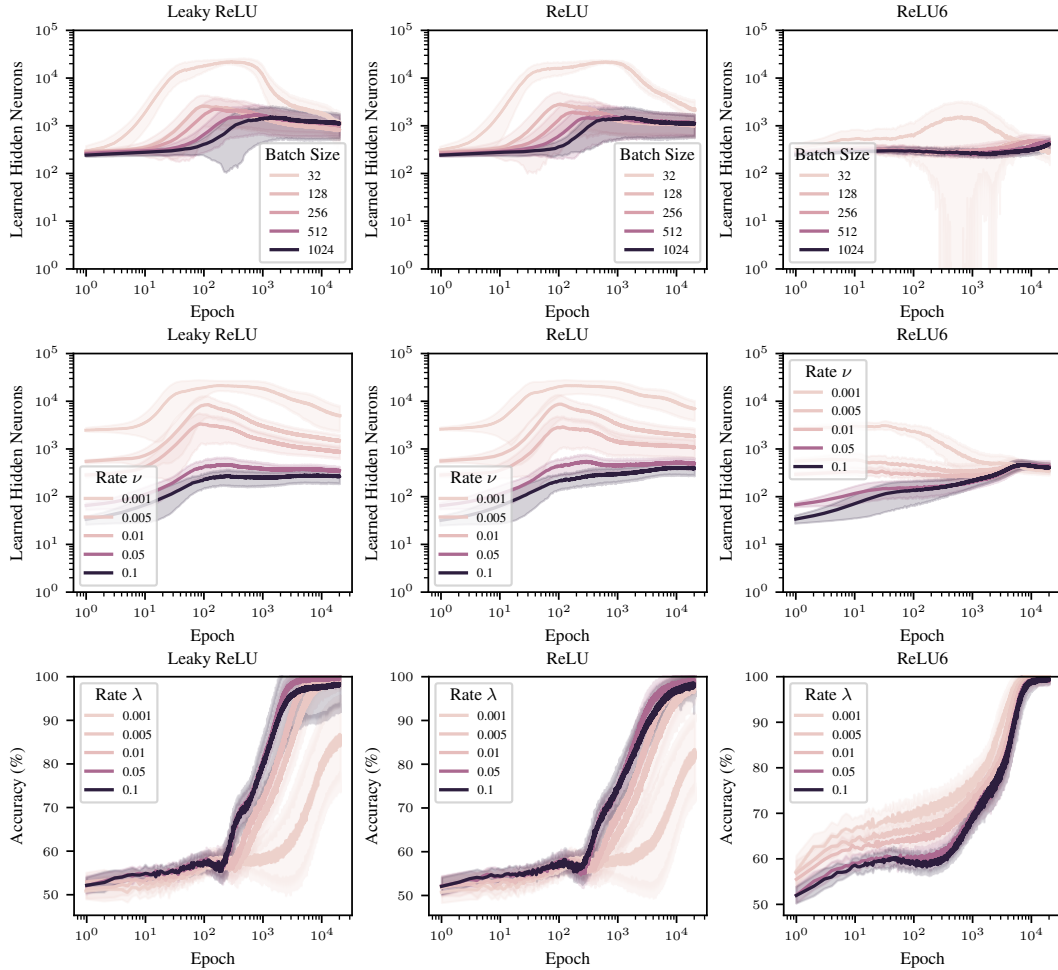


Figure 10: Impact of different batch sizes and starting exponential rates  $\lambda$ , organized by type of non-linear activation function.

These qualitative analyses support our claims that using a bounded activation is one way to encourage the network not to counterbalance the learned rescaling of each neuron. In fact, using a ReLU6 shows a distinctive convergence to the same amount of neurons among all configurations tried. The decreasing trend for LeakyReLU and ReLU activations may suggest that these configurations are also converging to a similar value than ReLU6, but they are taking a much longer time.

## K Learned width for each layer on Graph Datasets

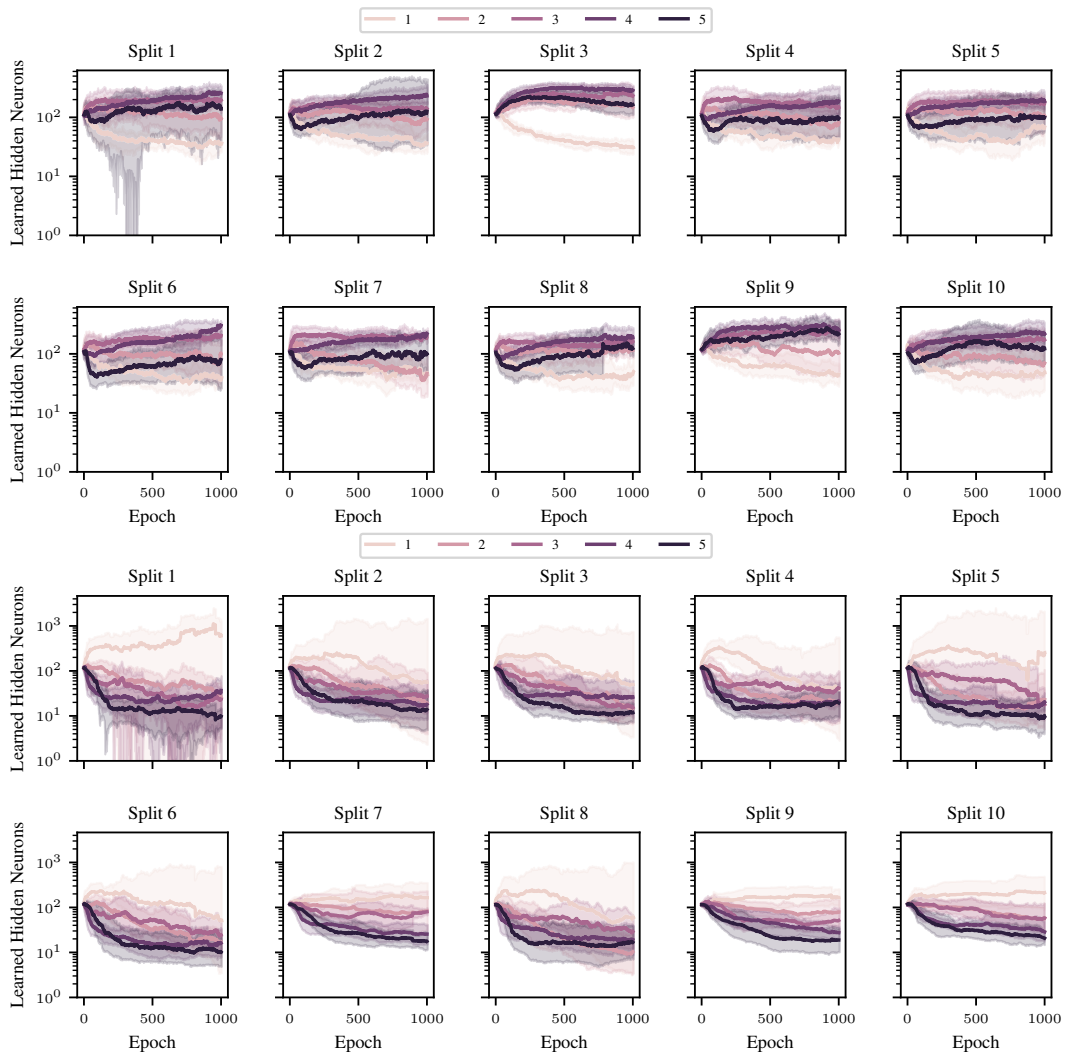


Figure 11: Learned neurons per layer (from 1 to 5), averaged over 10 final runs for each of the 10 best configurations selected in the outer folds. The first and second rows refer to NCI1, the third and fourth refer to REDDIT-B. One can observe similar trends in most cases.

## L Comparison with Neural Architecture Search (NAS)

Although complementary to our approach, we thought instructive to run some basic NAS methods on the image classification datasets. Most NAS methods fix an upper bound on the maximum width, whereas AWNN’s methodology does not. The truncation ability of AWNN is not intended as a substitute for pruning but rather as a confirmation of our claims. In fact, NAS and pruning can actually be combined with AWNN and do not necessarily be seen as “competing” strategies.

The results are shown in Table 6. That said, we compared the performance of AWNN against simple NAS methods on the vision datasets. We tested grid search, random search (Following Wu et al. [64]), local search [60], and Bayesian Optimization [1], fixing the same budget of 5 for all methods and width values between 0 (Linear classifier) and 512 neurons. Results are comparable to those of AWNN.

Table 6: Comparison between different NAS approaches and AWNN. We remind the reader that NAS is an orthogonal and complementary research direction to AWNN.

	Grid Search	Random Search	Local Search	Bayes. Optim.	AWNN
MNIST	99.6(0.1)	99.6(0.0)	99.5	99.4	99.7(0.0)
CIFAR10	91.4(0.2)	90.1(0.5)	90.6	91.2	91.4(0.2)
CIFAR100	66.5(0.4)	64.9(1.1)	64.9	65.9	63.1(4.0)

## NeurIPS Paper Checklist

### 1. Claims

Question: Do the main claims made in the abstract and introduction accurately reflect the paper's contributions and scope?

Answer: [\[Yes\]](#)

Justification: Abstract and introduction reflect our results.

Guidelines:

- The answer NA means that the abstract and introduction do not include the claims made in the paper.
- The abstract and/or introduction should clearly state the claims made, including the contributions made in the paper and important assumptions and limitations. A No or NA answer to this question will not be perceived well by the reviewers.
- The claims made should match theoretical and experimental results, and reflect how much the results can be expected to generalize to other settings.
- It is fine to include aspirational goals as motivation as long as it is clear that these goals are not attained by the paper.

### 2. Limitations

Question: Does the paper discuss the limitations of the work performed by the authors?

Answer: [\[Yes\]](#)

Justification: Section 3.3 discusses limitations and future extensions.

Guidelines:

- The answer NA means that the paper has no limitation while the answer No means that the paper has limitations, but those are not discussed in the paper.
- The authors are encouraged to create a separate "Limitations" section in their paper.
- The paper should point out any strong assumptions and how robust the results are to violations of these assumptions (e.g., independence assumptions, noiseless settings, model well-specification, asymptotic approximations only holding locally). The authors should reflect on how these assumptions might be violated in practice and what the implications would be.
- The authors should reflect on the scope of the claims made, e.g., if the approach was only tested on a few datasets or with a few runs. In general, empirical results often depend on implicit assumptions, which should be articulated.
- The authors should reflect on the factors that influence the performance of the approach. For example, a facial recognition algorithm may perform poorly when image resolution is low or images are taken in low lighting. Or a speech-to-text system might not be used reliably to provide closed captions for online lectures because it fails to handle technical jargon.
- The authors should discuss the computational efficiency of the proposed algorithms and how they scale with dataset size.
- If applicable, the authors should discuss possible limitations of their approach to address problems of privacy and fairness.
- While the authors might fear that complete honesty about limitations might be used by reviewers as grounds for rejection, a worse outcome might be that reviewers discover limitations that aren't acknowledged in the paper. The authors should use their best judgment and recognize that individual actions in favor of transparency play an important role in developing norms that preserve the integrity of the community. Reviewers will be specifically instructed to not penalize honesty concerning limitations.

### 3. Theory assumptions and proofs

Question: For each theoretical result, does the paper provide the full set of assumptions and a complete (and correct) proof?

Answer: [\[Yes\]](#)

Justification: All theorems in the appendix come with a complete proof with the necessary assumptions.

Guidelines:

- The answer NA means that the paper does not include theoretical results.
- All the theorems, formulas, and proofs in the paper should be numbered and cross-referenced.
- All assumptions should be clearly stated or referenced in the statement of any theorems.
- The proofs can either appear in the main paper or the supplemental material, but if they appear in the supplemental material, the authors are encouraged to provide a short proof sketch to provide intuition.
- Inversely, any informal proof provided in the core of the paper should be complemented by formal proofs provided in appendix or supplemental material.
- Theorems and Lemmas that the proof relies upon should be properly referenced.

#### 4. Experimental result reproducibility

Question: Does the paper fully disclose all the information needed to reproduce the main experimental results of the paper to the extent that it affects the main claims and/or conclusions of the paper (regardless of whether the code and data are provided or not)?

Answer: [Yes]

Justification: The paper provides experimental details about the datasets, data splits, and hyper-parameters tried in the appendix. Also, the experiments are easy to reproduce thanks to the adoption of ad-hoc libraries in the supplementary material.

Guidelines:

- The answer NA means that the paper does not include experiments.
- If the paper includes experiments, a No answer to this question will not be perceived well by the reviewers: Making the paper reproducible is important, regardless of whether the code and data are provided or not.
- If the contribution is a dataset and/or model, the authors should describe the steps taken to make their results reproducible or verifiable.
- Depending on the contribution, reproducibility can be accomplished in various ways. For example, if the contribution is a novel architecture, describing the architecture fully might suffice, or if the contribution is a specific model and empirical evaluation, it may be necessary to either make it possible for others to replicate the model with the same dataset, or provide access to the model. In general, releasing code and data is often one good way to accomplish this, but reproducibility can also be provided via detailed instructions for how to replicate the results, access to a hosted model (e.g., in the case of a large language model), releasing of a model checkpoint, or other means that are appropriate to the research performed.
- While NeurIPS does not require releasing code, the conference does require all submissions to provide some reasonable avenue for reproducibility, which may depend on the nature of the contribution. For example
  - (a) If the contribution is primarily a new algorithm, the paper should make it clear how to reproduce that algorithm.
  - (b) If the contribution is primarily a new model architecture, the paper should describe the architecture clearly and fully.
  - (c) If the contribution is a new model (e.g., a large language model), then there should either be a way to access this model for reproducing the results or a way to reproduce the model (e.g., with an open-source dataset or instructions for how to construct the dataset).
  - (d) We recognize that reproducibility may be tricky in some cases, in which case authors are welcome to describe the particular way they provide for reproducibility. In the case of closed-source models, it may be that access to the model is limited in some way (e.g., to registered users), but it should be possible for other researchers to have some path to reproducing or verifying the results.

#### 5. Open access to data and code

Question: Does the paper provide open access to the data and code, with sufficient instructions to faithfully reproduce the main experimental results, as described in supplemental material?

Answer: [Yes]

Justification: Yes, see also our previous answer.

Guidelines:

- The answer NA means that paper does not include experiments requiring code.
- Please see the NeurIPS code and data submission guidelines (<https://nips.cc/public/guides/CodeSubmissionPolicy>) for more details.
- While we encourage the release of code and data, we understand that this might not be possible, so “No” is an acceptable answer. Papers cannot be rejected simply for not including code, unless this is central to the contribution (e.g., for a new open-source benchmark).
- The instructions should contain the exact command and environment needed to run to reproduce the results. See the NeurIPS code and data submission guidelines (<https://nips.cc/public/guides/CodeSubmissionPolicy>) for more details.
- The authors should provide instructions on data access and preparation, including how to access the raw data, preprocessed data, intermediate data, and generated data, etc.
- The authors should provide scripts to reproduce all experimental results for the new proposed method and baselines. If only a subset of experiments are reproducible, they should state which ones are omitted from the script and why.
- At submission time, to preserve anonymity, the authors should release anonymized versions (if applicable).
- Providing as much information as possible in supplemental material (appended to the paper) is recommended, but including URLs to data and code is permitted.

## 6. Experimental setting/details

Question: Does the paper specify all the training and test details (e.g., data splits, hyper-parameters, how they were chosen, type of optimizer, etc.) necessary to understand the results?

Answer: [Yes]

Justification: Yes, see also our previous answers.

Guidelines:

- The answer NA means that the paper does not include experiments.
- The experimental setting should be presented in the core of the paper to a level of detail that is necessary to appreciate the results and make sense of them.
- The full details can be provided either with the code, in appendix, or as supplemental material.

## 7. Experiment statistical significance

Question: Does the paper report error bars suitably and correctly defined or other appropriate information about the statistical significance of the experiments?

Answer: [Yes]

Justification: See Table 1.

Guidelines:

- The answer NA means that the paper does not include experiments.
- The authors should answer "Yes" if the results are accompanied by error bars, confidence intervals, or statistical significance tests, at least for the experiments that support the main claims of the paper.
- The factors of variability that the error bars are capturing should be clearly stated (for example, train/test split, initialization, random drawing of some parameter, or overall run with given experimental conditions).
- The method for calculating the error bars should be explained (closed form formula, call to a library function, bootstrap, etc.)

- The assumptions made should be given (e.g., Normally distributed errors).
- It should be clear whether the error bar is the standard deviation or the standard error of the mean.
- It is OK to report 1-sigma error bars, but one should state it. The authors should preferably report a 2-sigma error bar than state that they have a 96% CI, if the hypothesis of Normality of errors is not verified.
- For asymmetric distributions, the authors should be careful not to show in tables or figures symmetric error bars that would yield results that are out of range (e.g. negative error rates).
- If error bars are reported in tables or plots, The authors should explain in the text how they were calculated and reference the corresponding figures or tables in the text.

## 8. Experiments compute resources

Question: For each experiment, does the paper provide sufficient information on the computer resources (type of compute workers, memory, time of execution) needed to reproduce the experiments?

Answer: [Yes]

Justification: See Section 4.

Guidelines:

- The answer NA means that the paper does not include experiments.
- The paper should indicate the type of compute workers CPU or GPU, internal cluster, or cloud provider, including relevant memory and storage.
- The paper should provide the amount of compute required for each of the individual experimental runs as well as estimate the total compute.
- The paper should disclose whether the full research project required more compute than the experiments reported in the paper (e.g., preliminary or failed experiments that didn't make it into the paper).

## 9. Code of ethics

Question: Does the research conducted in the paper conform, in every respect, with the NeurIPS Code of Ethics <https://neurips.cc/public/EthicsGuidelines?>

Answer: [Yes]

Justification: Our approach is a general machine learning methodology that could be used in unforeseen ways. We did not experiment on human subjects and the data is publicly available.

Guidelines:

- The answer NA means that the authors have not reviewed the NeurIPS Code of Ethics.
- If the authors answer No, they should explain the special circumstances that require a deviation from the Code of Ethics.
- The authors should make sure to preserve anonymity (e.g., if there is a special consideration due to laws or regulations in their jurisdiction).

## 10. Broader impacts

Question: Does the paper discuss both potential positive societal impacts and negative societal impacts of the work performed?

Answer: [NA]

Justification: No societal impact of the work performed.

Guidelines:

- The answer NA means that there is no societal impact of the work performed.
- If the authors answer NA or No, they should explain why their work has no societal impact or why the paper does not address societal impact.
- Examples of negative societal impacts include potential malicious or unintended uses (e.g., disinformation, generating fake profiles, surveillance), fairness considerations (e.g., deployment of technologies that could make decisions that unfairly impact specific groups), privacy considerations, and security considerations.

- The conference expects that many papers will be foundational research and not tied to particular applications, let alone deployments. However, if there is a direct path to any negative applications, the authors should point it out. For example, it is legitimate to point out that an improvement in the quality of generative models could be used to generate deepfakes for disinformation. On the other hand, it is not needed to point out that a generic algorithm for optimizing neural networks could enable people to train models that generate Deepfakes faster.
- The authors should consider possible harms that could arise when the technology is being used as intended and functioning correctly, harms that could arise when the technology is being used as intended but gives incorrect results, and harms following from (intentional or unintentional) misuse of the technology.
- If there are negative societal impacts, the authors could also discuss possible mitigation strategies (e.g., gated release of models, providing defenses in addition to attacks, mechanisms for monitoring misuse, mechanisms to monitor how a system learns from feedback over time, improving the efficiency and accessibility of ML).

## 11. Safeguards

Question: Does the paper describe safeguards that have been put in place for responsible release of data or models that have a high risk for misuse (e.g., pretrained language models, image generators, or scraped datasets)?

Answer: [NA]

Justification: No such risks.

Guidelines:

- The answer NA means that the paper poses no such risks.
- Released models that have a high risk for misuse or dual-use should be released with necessary safeguards to allow for controlled use of the model, for example by requiring that users adhere to usage guidelines or restrictions to access the model or implementing safety filters.
- Datasets that have been scraped from the Internet could pose safety risks. The authors should describe how they avoided releasing unsafe images.
- We recognize that providing effective safeguards is challenging, and many papers do not require this, but we encourage authors to take this into account and make a best faith effort.

## 12. Licenses for existing assets

Question: Are the creators or original owners of assets (e.g., code, data, models), used in the paper, properly credited and are the license and terms of use explicitly mentioned and properly respected?

Answer: [No]

Justification: We do rely on Python packages but did not acknowledge each of them in our paper.

Guidelines:

- The answer NA means that the paper does not use existing assets.
- The authors should cite the original paper that produced the code package or dataset.
- The authors should state which version of the asset is used and, if possible, include a URL.
- The name of the license (e.g., CC-BY 4.0) should be included for each asset.
- For scraped data from a particular source (e.g., website), the copyright and terms of service of that source should be provided.
- If assets are released, the license, copyright information, and terms of use in the package should be provided. For popular datasets, [paperswithcode.com/datasets](https://paperswithcode.com/datasets) has curated licenses for some datasets. Their licensing guide can help determine the license of a dataset.
- For existing datasets that are re-packaged, both the original license and the license of the derived asset (if it has changed) should be provided.

- If this information is not available online, the authors are encouraged to reach out to the asset’s creators.

### 13. **New assets**

Question: Are new assets introduced in the paper well documented and is the documentation provided alongside the assets?

Answer: [Yes]

Justification: See the supplementary material.

Guidelines:

- The answer NA means that the paper does not release new assets.
- Researchers should communicate the details of the dataset/code/model as part of their submissions via structured templates. This includes details about training, license, limitations, etc.
- The paper should discuss whether and how consent was obtained from people whose asset is used.
- At submission time, remember to anonymize your assets (if applicable). You can either create an anonymized URL or include an anonymized zip file.

### 14. **Crowdsourcing and research with human subjects**

Question: For crowdsourcing experiments and research with human subjects, does the paper include the full text of instructions given to participants and screenshots, if applicable, as well as details about compensation (if any)?

Answer: [NA]

Justification: No research on human subjects.

Guidelines:

- The answer NA means that the paper does not involve crowdsourcing nor research with human subjects.
- Including this information in the supplemental material is fine, but if the main contribution of the paper involves human subjects, then as much detail as possible should be included in the main paper.
- According to the NeurIPS Code of Ethics, workers involved in data collection, curation, or other labor should be paid at least the minimum wage in the country of the data collector.

### 15. **Institutional review board (IRB) approvals or equivalent for research with human subjects**

Question: Does the paper describe potential risks incurred by study participants, whether such risks were disclosed to the subjects, and whether Institutional Review Board (IRB) approvals (or an equivalent approval/review based on the requirements of your country or institution) were obtained?

Answer: [NA]

Justification: No research on human subjects.

Guidelines:

- The answer NA means that the paper does not involve crowdsourcing nor research with human subjects.
- Depending on the country in which research is conducted, IRB approval (or equivalent) may be required for any human subjects research. If you obtained IRB approval, you should clearly state this in the paper.
- We recognize that the procedures for this may vary significantly between institutions and locations, and we expect authors to adhere to the NeurIPS Code of Ethics and the guidelines for their institution.
- For initial submissions, do not include any information that would break anonymity (if applicable), such as the institution conducting the review.

### 16. **Declaration of LLM usage**

Question: Does the paper describe the usage of LLMs if it is an important, original, or non-standard component of the core methods in this research? Note that if the LLM is used only for writing, editing, or formatting purposes and does not impact the core methodology, scientific rigorousness, or originality of the research, declaration is not required.

Answer: [NA]

Justification: The core method development in this research does not involve LLMs as any important, original, or non-standard components.

Guidelines:

- The answer NA means that the core method development in this research does not involve LLMs as any important, original, or non-standard components.
- Please refer to our LLM policy (<https://neurips.cc/Conferences/2025/LLM>) for what should or should not be described.